through transduction of genes encoding immunofunctional molecules as well as for antigen gene delivery into DCs.

The immune system is roughly classified into cellular immunity and humoral immunity, and optimal immune response is achieved by balanced activation of both systems. Cellular immune response, based on the activation of natural killer (NK) cells and TAA-specific cytotoxic T lymphocytes (CTLs), plays a more important role in elimination of tumor cells by tumor immunity than humoral immune response accompanied by antibody production from B cells.[10–13] Therefore, an approach that biases immune balance toward the cellular immune response would enhance the efficacy of DC-based immunotherapy for cancer. Interleukin (IL)-12 is a 70 kDa (p70) heterodimer protein in which the 40 kDa (p40) and 35 kDa (p35) subunits are connected by one S–S bond.[14,15] IL-12 plays a key role in the induction of cellular immune responses, such as enhancement of proliferation and cytotoxic activity in NK cells and CTLs,[16,17] production of interferon (IFN)-γ from activated cells,[17–19] and promotion of differentiation of helper T-type 1 (Th1) cells from Th0 cells.[17,20,21] IFN-γ is involved in IL-12-mediated tumor regression,[22] and IL-12 also exhibits an antiangiogenic effect that can account for some antitumor activity.[23] Thus, it was strongly predicted that DCs cotransduced with the TAA and IL-12 genes may be efficacious vaccine carriers that can drastically improve effectiveness of DC-based immunotherapy for cancer by positively biasing immune balance toward cellular immunity, the Th1-dominant state, by inducing IL-12 secretion as well as by sensitizing TAA-specific CTLs via TAA-peptide presentation on major histocompatibility complex (MHC) molecules.

In the present study, by using AdRGD, which is superior in gene transduction efficiency to DCs, we created a DC vaccine that simultaneously expressed gp100, a melanoma-associated antigen, and IL-12, and investigated its immunological characteristics and vaccine efficacy.

Materials and methods

Cell lines and mice

The helper cell line, 293 cells, was obtained from JCRB cell bank (Tokyo, Japan) and cultured in Dulbecco's modified Eagle's medium supplemented with 10% fetal bovine serum (FBS) and antibiotics. CD8-OVA 1.3 cells,[24] a specific T–T hybridoma against ovalbumin (OVA)$^+$ H-2K^b (kindly provided by Dr CV Harding; Department of Pathology, Case Western Reserve University, Cleveland, OH), were maintained in Dulbecco's modified Eagle's medium supplemented with 10% FBS, 50 μM 2-mercaptoethanol (2-ME), and antibiotics. Murine melanoma B16BL6 cells (H-2^b; JCRB cell bank) were grown in minimum essential medium supplemented with 7.5% FBS and antibiotics. EL4 cells, a T-lymphoma cell line of C57BL/6 origin, and YAC-1 cells, a lymphoma cell line highly sensitive to NK cells, were purchased from ATCC (Manassas, VA) and maintained in RPMI 1640 medium supplemented with 10% FBS, 50 μM 2-ME, and antibiotics. Female C57BL/6 mice (H-2^b) and female BALB/c mice (H-2^d), ages 7–8 weeks, were purchased from SLC Inc. (Hamamatsu, Japan). All mice were held under specific pathogen-free conditions and the experimental procedures were in accordance with the Osaka University guidelines for the welfare of animals in experimental neoplasia.

Vectors

Replication-deficient AdRGD was based on the adenovirus serotype 5 backbone with deletions of regions E1 and E3. The RGD sequence for αv-integrin-targeting was inserted into the HI loop of the fiber knob using a two-step method as previously described.[25] AdRGD-IL12,[26] AdRGD-gp100,[7] AdRGD-OVA,[8] and AdRGD-Luc[25] were previously constructed by an improved *in vitro* ligation method,[25,27,28] and encoded the murine IL-12 gene derived from mIL12 BIA/pBluescript II KS(-) (kindly provided by Dr H Yamamoto; Department of Immunology, Graduate School of Pharmaceutical Sciences, Osaka University, Suita, Japan), the human gp100 gene derived from pAx1-CA h-gp100 (kindly provided by Dr H Hamada; Department of Molecular Medicine, Sapporo Medical University, Sapporo, Japan), the OVA gene derived from pAc-neo-OVA (kindly provided by Dr MJ Bevan; Department of Immunology, Howard Hughes Medical Institute, University of Washington, Seattle, WA), and the luciferase gene derived from pGL3-Control (Promega, Madison, WI), respectively. All recombinant AdRGDs were propagated in 293 cells, purified by two rounds of cesium chloride gradient ultracentrifugation, dialyzed, and stored at −80°C. Titers of infective AdRGD particles were evaluated by the end point dilution method using 293 cells.

Generation and viral transduction of DCs

DCs were prepared according to the method of Lutz et al[29] with slight modification. Briefly, bone marrow cells flushed from the femurs and tibias of C57BL/6 mice were seeded at 0.5–1 $\times$ 10^7 cells per sterile 100-mm bacterial grade culture dish in 10 ml of RPMI 1640 containing 10% FBS, 40 ng/ml recombinant murine granulocyte/macrophage colony-stimulating factor (GM-CSF; kindly provided by KIRIN Brewery Co., LTD, Tokyo, Japan), 50 μM 2-ME, and antibiotics. On day 3, another 10 ml of culture medium was added to the dish for medium replenishment. On day 6, 10 ml of the culture supernatant was collected and centrifuged at 1500 rpm for 5 minutes at room temperature, and the pellet was resuspended in 10 ml of fresh culture medium, and then returned to the original dish to conserve unattached cells. On day 8, nonadherent cells were harvested and used as immature DCs. DCs cultured for another 24 hours with media containing 1 μg/ml lipopolysaccharide (LPS; Nacalai Tesque, Inc., Kyoto, Japan) were used as phenotypically mature DCs (LPS/DCs). In transduction using AdRGDs,

DCs were suspended at a concentration of 5×10^6 cells/ml in FBS-free RPMI 1640 and placed in a 15-ml conical tube. Each AdRGD was added at various multiplicity of infections (MOIs), the suspension was mixed well, and the tube was incubated at 37°C for 2 hours with occasional gentle agitation. The cells were washed three times with phosphate-buffered saline (PBS) and resuspended in a suitable solution for subsequent experiments.

Reverse transcription-polymerase chain reaction (RT-PCR) analysis

Transduced DCs and mock DCs were cultured on 100-mm bacterial grade culture dishes in GM-CSF-free culture medium for 24 hours. Total RNA was isolated from these cells and LPS/DCs using Sepasol-RNA I Super (Nacalai Tesque, Inc.) according to the manufacturer's instructions. RT proceeded for 60 minutes at 42°C in a 50 μl reaction mixture containing 5 μg total RNA treated with DNase I, 10 μl 5 × RT buffer, 5 mM $MgCl_2$, 1 mM dNTP mix, 1 μM random primer (9-mer), 1 μM oligo$(dT)_{20}$, and 100 U ReverTra Ace (TOYOBO Co., LTD, Osaka, Japan). PCR amplification of the gp100, IL-12p35, IL-12p40, and β-actin transcripts was performed in 50 μl of a reaction mixture containing 1 μl of RT-material, 5 μl 10 × PCR buffer, 1.25 U *Taq* DNA polymerase (TOYOBO Co., LTD), 1.5 mM $MgCl_2$, 0.2 mM dNTP, and 0.4 μM primers. The sequences of the specific primers were as follows: human gp100: forward, 5′-tgg aac agg cag ctg tat cc-3′; reverse, 5′-cct aga act tgc cag tat tgg c-3′; murine IL-12p35: forward, 5′-tgt tta cca ctg gaa cta cac aag a-3′; reverse, 5′-aga gct tca ttt tca ctc tgt aag g-3′; murine IL-12p40: forward, 5′-ctc acc tgt gac acg cct ga-3′; reverse, 5′-cag gac act gaa tac ttc tc-3′; murine β-actin: forward, 5′-tgt gat ggt ggg aat ggg tca g-3′; reverse, 5′-ttt gat gtc acg cac gat ttc c-3′. After denaturation for 2 minutes at 95°C, 20 cycles of denaturation for 30 seconds at 95°C, annealing for 30 seconds at 48°C (for IL-12p40), 58°C (for IL-12p35), or 60°C (for gp100 and β-actin), and extension for 30 seconds at 72°C were repeated and followed by completion for 4 minutes at 72°C. The PCR product was electrophoresed on a 3% agarose gel, stained with ethidium bromide, and visualized under ultraviolet radiation. EZ Load (BIO-RAD, Tokyo, Japan) was used as a 100 bp-molecular ruler. The expected PCR product sizes were 362 bp (gp100), 334 bp (IL-12p35), 431 bp (IL-12p40), and 514 bp (β-actin).

Intracellular staining method for human gp100 protein in transduced DCs

Transduced DCs were cultured on 100-mm bacterial grade culture dishes in GM-CSF-free culture medium for 24 hours. Cells (1×10^6) were fixed by incubation for 10 minutes in 2% paraformaldehyde, and then cell membranes were permeabilized by incubation for 5 minutes in 1% saponin. The cells were incubated with 100 μl staining buffer (PBS containing 0.1% bovine serum albumin and 0.01% NaN_3) containing the anti-FcγRII/III monoclonal antibody (mAb), 2.4G2 (rat $IgG_{2b,\kappa}$; BD Biosciences, San Jose, CA), to block nonspecific binding of the subsequently used mAbs. After 30 minutes, the cells were incubated for 60 minutes with 100 μl staining buffer containing the HMB50 mAb against human gp100 (mouse IgG_{2a}; Neomarkers, Fremont, CA), and then resuspended in 100 μl staining buffer containing fluorescein isothiocyanate-conjugated anti-mouse Ig_κ (187.1; BD Biosciences). After incubation for 30 minutes, 30,000 events of the stained cells were analyzed for human gp100 protein expression by a FACScalibur flow cytometer using CellQuest software (BD Biosciences). Between all incubation steps, cells were washed three times with staining buffer.

Evaluation of IL-12 secretion level in transduced DCs

Transduced DCs, LPS/DCs, and mock DCs were cultured on 24-well plates at 5×10^5 cells/500 μl in GM-CSF-free culture medium for 24 hours. The supernatants were collected and the IL-12 level was measured using a murine IL-12p40 ELISA KIT and a murine IL-12p70 ELISA KIT (Endogen, Rockford, IL).

Analysis of surface marker-expression

All immunoreagents used in this experiment were purchased from BD Biosciences. Transduced DCs, LPS/DCs, and mock DCs were cultured on 100-mm bacterial grade culture dishes in GM-CSF-free culture medium for 24 hours. Cells (1×10^6) in 100 μl staining buffer were incubated for 30 minutes on ice with the 2.4G2 mAb. Then, cells were resuspended in 100 μl staining buffer and incubated for 30 minutes on ice using the manufacturer's recommended amounts of biotinylated mAbs: 28-8-6 (anti-H-$2K^b$/D^b), AF6-120.1 (anti-I-A^b), 3/23 (anti-CD40), 16-10A1 (anti-CD80), and GL1 (anti-CD86). The cells were then resuspended in 100 μl staining buffer containing phycoerythrin-conjugated streptavidin at a 1:200 dilution, and nonspecific binding was measured using phycoerythrin-conjugated streptavidin alone. After incubation for 30 minutes on ice, 30,000 events of the stained cells were analyzed for surface phenotype by flow cytometry. Between all incubation steps, cells were washed three times with staining buffer.

Antigen-presentation assay

C57BL/6 DCs were transduced with various combinations of AdRGD-OVA, AdRGD-IL12, and AdRGD-Luc, and then seeded on a 96-well flat-bottom culture plate at a density of 1×10^5 cells/well. These cells were cocultured with 1×10^5 cells/well CD8-OVA 1.3 cells at 37°C for 20 hours. The response of stimulated CD8-OVA 1.3 cells was assessed by determining the amount of IL-2 released into an aliquot of culture medium (100 μl) using a murine IL-2 ELISA KIT (Amersham Biosciences, Piscataway, NJ).

Mixed leukocyte reaction (MLR)

Three kinds of T cells, including allogeneic naive T cells from intact BALB/c mice, syngeneic naive T cells from intact C57BL/6 mice, and syngeneic gp100-primed T cells

from C57BL/6 mice immunized intradermally with 1×10^6 DCs transduced with AdRGD-gp100 at 25 MOI 1 week earlier, were purified from the splenocytes of each mouse as nylon wool nonadherent cells, and were used as responder cells at 1×10^5 cells/well in 96-well plates. Transduced DCs, LPS/DCs, or mock DCs (stimulator cells) were inactivated by 50 μg/ml mitomycin C (MMC) for 30 minutes and added to responder cells in varying cell numbers. Cells were cocultured in 100 μl RPMI 1640 supplemented with 10% FBS, 50 μM 2-ME, and antibiotics at 37°C and 5% CO_2 for 3 days. Control wells contained either stimulator cells alone or responder cells alone. Cell cultures were pulsed with 5-bromo-2′-deoxyuridine (BrdU) during the last 18 hours, and then proliferation of responder cells was evaluated by Cell Proliferation ELISA, BrdU (Roche Diagnostics Co., Indianapolis, IN).

Analysis of Th1/Th2 cytokine secretion from syngeneic T cells stimulated by transduced DCs

C57BL/6 naive T cells were purified from splenocytes as nylon wool nonadherent cells, and were used as responder cells at 5×10^6 cells/well in 24-well plates. Transduced DCs (stimulator cells) were added to responder cells at 5×10^5 cells/well. Cells were cocultured in 1 ml RPMI 1640 supplemented with 10% FBS, 50 μM 2-ME, 10 U/ml recombinant murine IL-2 (PeproTech EC LTD, London, England) and antibiotics at 37°C and 5% CO_2 for 5 days. The supernatants were collected and the IFN-γ, IL-4, and IL-10 levels were measured using a murine IFN-γ ELISA KIT, a murine IL-4 ELISA KIT, and a murine IL-10 ELISA KIT (Biosource International, Camarillo, CA), respectively.

Tumor protection assay

Transduced DCs were intradermally injected into the left flank of C57BL/6 mice at 2×10^5 cells/50 μl. At 1 week after the vaccination, 2×10^5 B16BL6 melanoma cells were intradermally inoculated into the right flank of the mice. The major and minor axes of the tumor were measured using microcalipers, and the tumor volume was calculated by the following formula: (tumor volume; mm^3) = (major axis; mm) × (minor axis; mm)^2 × 0.5236. The mice were euthanized when one of the two measurements was greater than 20 mm.

Europium (Eu)-release assay for cytolytic activity of NK cells and CTLs

Transduced or mock DCs were administered once intradermally into C57BL/6 mice at 2×10^5 cells/50 μl. At 1 week after immunization, nonadherent splenocytes were prepared from these mice and directly used as NK effector cells. The splenocytes were restimulated *in vitro* using B16BL6 cells, which were cultured in media containing 100 U/ml recombinant murine IFN-γ (PeproTech EC LTD) for 24 hours and inactivated with 50 μg/ml MMC at 37°C for 30 minutes, at an effector:stimulator ratio of 10:1 in RPMI 1640 supplemented with 10% FBS, 50 μM 2-ME, and antibiotics. After 5 days, the splenocytes were collected and used as CTL effector cells. Target cells (YAC-1 and EL4 cells for NK assay; IFN-γ-stimulated B16BL6 and IFN-γ-stimulated EL4 cells for CTL assay) were Eu-labeled and an Eu-release assay was performed as previously described.[30] Cytolytic activity was determined using the following formula: (% of lysis) = [(experimental Eu-release − spontaneous Eu-release)/(maximum Eu-release − spontaneous Eu-release)] × 100. Spontaneous Eu-release of the target cells was <10% of maximum Eu-release by detergent in all assays.

Results

Gene expression in DCs cotransduced with gp100 and IL-12

We examined the cytopathic effects of AdRGD-IL12 and AdRGD-gp100 on gene transduction into DCs by using the Cell Counting Kit-8 (DOJINDO LABORATORIES, Kumamoto, Japan). At 48 hours posttransduction, viability of DCs transduced with AdRGD-IL12 alone or AdRGD-IL12 plus AdRGD-gp100 remained more than 90% at a vector dose of 200 MOI or less (data not shown). Expression levels of human gp100 and murine IL-12 subunit mRNAs in various transduced DCs were analyzed by RT-PCR at 24 hours after gene transduction (Fig 1). Human gp100-specific PCR products were detected at the same level only in DCs that were transduced with AdRGD-gp100 alone at 25 MOI (lane 1) or the combination of AdRGD-gp100 at 25 MOI and AdRGD-IL12 at various MOI (lanes 3, 4, and 5). PCR

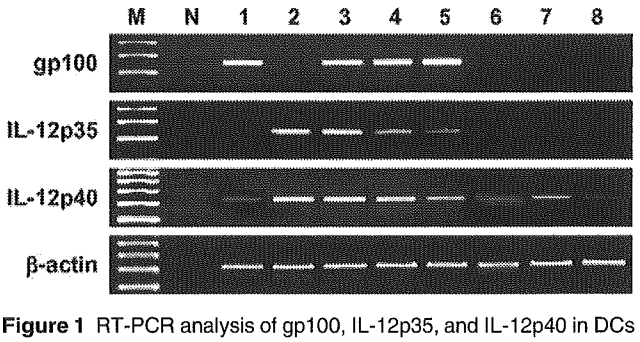

Figure 1 RT-PCR analysis of gp100, IL-12p35, and IL-12p40 in DCs cotransduced with AdRGD-gp100 and AdRGD-IL12. Total RNA was prepared from transduced, LPS-stimulated, or mock DCs, and then RT-PCR was performed as described in the Materials and methods section. The PCR products were electrophoresed through a 3% agarose gel, stained with ethidium bromide, and visualized under ultraviolet light. Lane M; 100 bp-molecular ruler, lane N; H_2O as template, lane 1; DCs transduced with AdRGD-gp100 alone at 25 MOI, lane 2; DCs transduced with AdRGD-IL12 alone at 25 MOI, lane 3; DCs cotransduced with AdRGD-gp100 at 25 MOI and AdRGD-IL12 at 25 MOI, lane 4; DCs cotransduced with AdRGD-gp100 at 25 MOI and AdRGD-IL12 at 12.5 MOI, lane 5; DCs cotransduced with AdRGD-gp100 at 25 MOI and AdRGD-IL12 at 5 MOI, lane 6; DCs transduced with AdRGD-Luc alone at 25 MOI, lane 7; LPS-stimulated (mature) DCs, lane 8; mock (immature) DCs.

products of IL-12p35 and IL-12p40 mRNA increased in an MOI-dependent manner for AdRGD-IL12 in DCs cotransduced with AdRGD-gp100 and AdRGD-IL12 (lanes 3, 4, and 5), and their levels were equal in DCs transduced with AdRGD-IL12 alone at 25 MOI (lane 2) and DCs cotransduced with AdRGD-gp100 at 25 MOI and AdRGD-IL12 at 25 MOI (lane 3). In addition, DCs transduced with AdRGD-gp100 alone (lane 1) or AdRGD-Luc (control vector) alone (lane 6) exhibited slightly higher IL-12p40 mRNA expression than mock DCs (lane 8), and IL-12p40 mRNA levels of LPS/DCs (lane 7) were comparable with those of DCs cotransduced with AdRGD-gp100 at 25 MOI and AdRGD-IL12 at 5 MOI (lane 5).

In order to confirm cytoplasmic expression of human gp100 protein, we performed flow cytometric analysis by the intracellular staining method using HMB50 mAb (Fig 2a). Under transductional conditions using AdRGD-gp100 at 25 MOI, about 70% of DCs could express gp100 protein in their cytoplasm whether or not the DCs were cotransduced individually with AdRGD-IL12 or AdRGD-Luc at 25 MOI. Gene expression intensity (mean fluorescence intensity; MFI) of gp100 in cotransduced DCs was also comparable to that of DCs transduced with AdRGD-gp100 alone. These data clearly demonstrated that the expression level of endogenous antigen transduced with AdRGD was not affected by cotransduction of AdRGD-IL12 in DCs. Likewise, IL-12 secretion levels in DCs transduced with various combinations of AdRGD-gp100 and AdRGD-IL12 were investigated by ELISA (Fig 2b). MOI-dependent IL-12p70, the biologically active form, and IL12p40 secretion into culture media of DCs cotransduced with AdRGD-gp100 and AdRGD-IL12 was detected at levels equivalent to those of DCs transduced with AdRGD-IL12 alone. Although LPS/DCs could secrete a large quantity of IL-12p40 into culture media, secretion of the active form, IL-12p70, was maintained at low levels, reflecting the low levels of IL-12p35 mRNA expression in RT-PCR analysis.

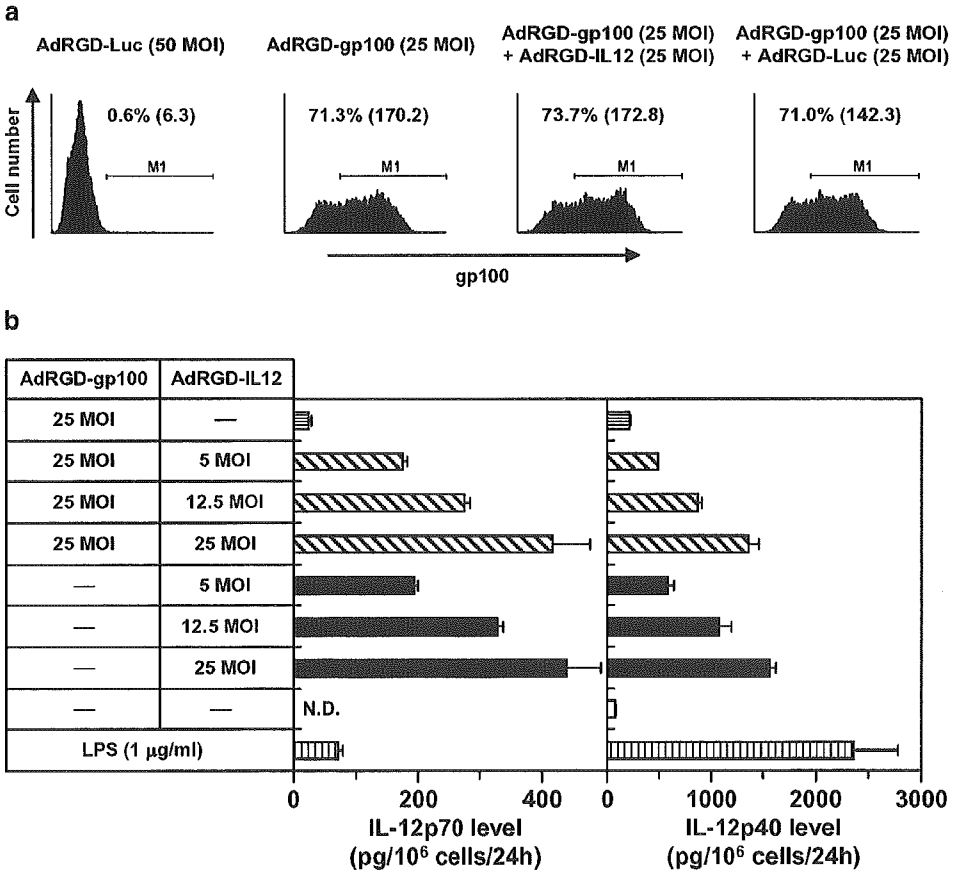

Figure 2 gp100 and IL-12 expression in DCs cotransduced with AdRGD-gp100 and AdRGD-IL12. (**a**) DCs were transduced with the indicated combinations of various AdRGDs at the indicated MOI for 2 hours. At 24 hours posttransduction, human gp100 gene expression was assessed by flow cytometric analysis. The percentage value and the numerical value in the parenthesis express percentage of M1-gated cells and mean fluorescence intensity (MFI), respectively. The data are representative of two independent experiments. (**b**) DCs were cotransduced with AdRGD-IL12 and AdRGD-gp100 at the indicated MOI for 2 hours. DCs treated with 1 μg/ml LPS for 24 hours were used as positive controls for phenotypical DC-maturation. After 24 hours cultivation, concentration of murine IL-12p70 and IL-12p40 in culture supernatants was measured by ELISA. The data are presented as mean $\pm$ SD of three independent cultures. ND: IL-12p70 secreted from DCs was not detectable.

Immunological characteristics of DCs cotransduced with gp100 and IL-12

We first analyzed the expression levels of MHC/costimulatory molecules by flow cytometry in DCs prepared with various combinations of AdRGD-gp100 and AdRGD-IL12 (Fig 3). In comparison with mock DCs, DCs transduced with AdRGD-gp100 alone exhibited upregulated expression of all tested surface marker molecules, which play critical roles in the sensitization/activation of T cells, as was seen in mature LPS/DCs. This result agreed with our previous report demonstrating that transduction using AdRGD, irrespective of the type of inserted transgene, could enhance the expression of MHC/costimulatory molecules on DCs.[7] In addition, enhanced expression of MHC class I, CD40 and CD86 was observed as a characteristic change in DCs cotransduced with AdRGD-gp100 and AdRGD-IL12 as well as DCs transduced with AdRGD-IL12 alone. As upregulation of these molecules was dependent on MOI of combined AdRGD-IL12, the results suggested that the secreted IL-12 promoted maturation of DCs by an autocrine mechanism.

Next, we compared antigen presentation levels via MHC class I molecules by bioassay using T–T hybridoma, CD8-OVA 1.3 cells, between DCs transduced with various combinations of AdRGD-OVA, AdRGD-IL12, and AdRGD-Luc (Fig 4). In comparison with DCs transduced with AdRGD-OVA alone, DCs cotransduced with AdRGD-OVA and AdRGD-IL12 showed a slight decrease in IL-2 released from CD8-OVA 1.3 cells by vector dose-increase of combined AdRGD-IL12. The OVA-presentation levels in AdRGD-OVA-transduced DCs were not affected by the addition of exogenous recombinant murine IL-12 into culture media during the antigen-presentation assay (data not shown). In addition, an obvious decline in the OVA-presentation level was observed in DCs cotransduced with AdRGD-OVA and AdRGD-Luc, suggesting that competition may occur during a particular step of the MHC class I

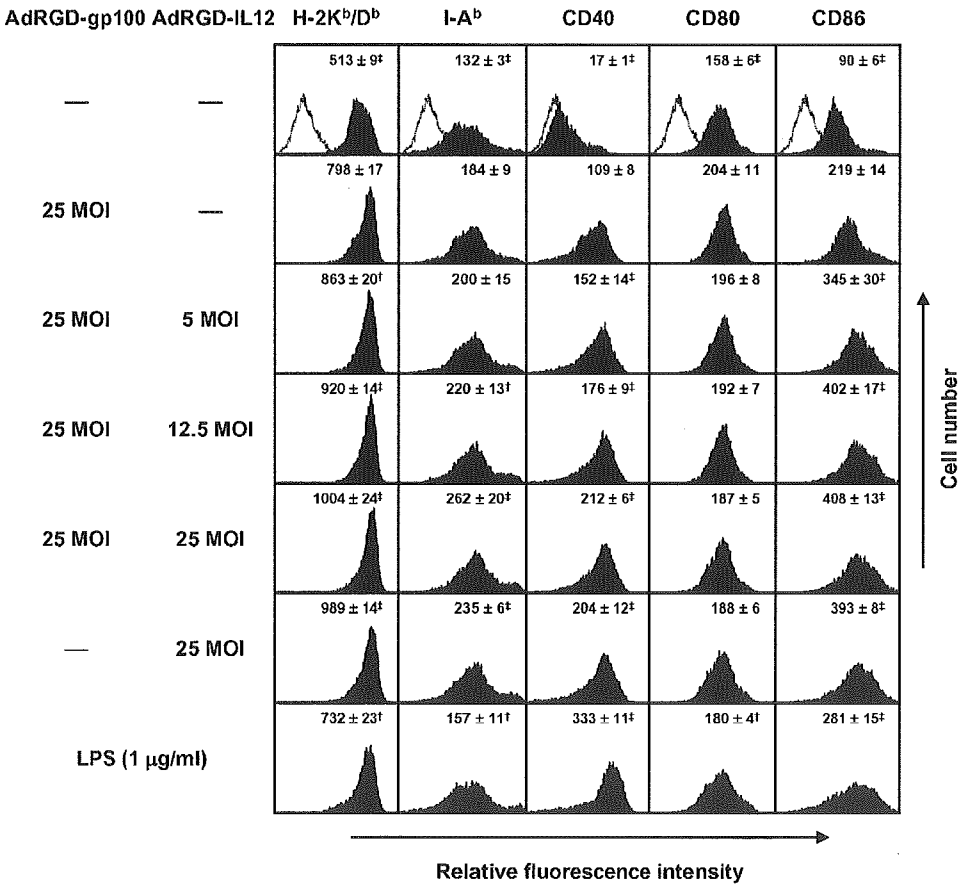

Figure 3 Flow cytometric analysis of surface markers in DCs cotransduced with gp100 and IL-12 gene by AdRGD. DCs were cotransduced with AdRGD-gp100 and AdRGD-IL12 at the indicated MOI for 2 hours. DCs treated with 1 μg/ml LPS for 24 hours were used as positive controls for phenotypical DC maturation. At 24 hours after transduction, cells were stained by indirect immunofluorescence using biotinylated mAbs of the indicated specificities (solid histogram). Dotted histograms represent cells stained by phycoerythrin-conjugated streptavidin alone. The data are representative of three independent experiments, and values indicated in the upper part of each panel represent MFI (mean ± SD) of flow cytometric analysis. The statistical analysis was carried out by Student's *t*-test. †$P<.05$, ‡$P<.01$ *versus* DCs transduced with AdRGD-gp100 alone at 25 MOI.

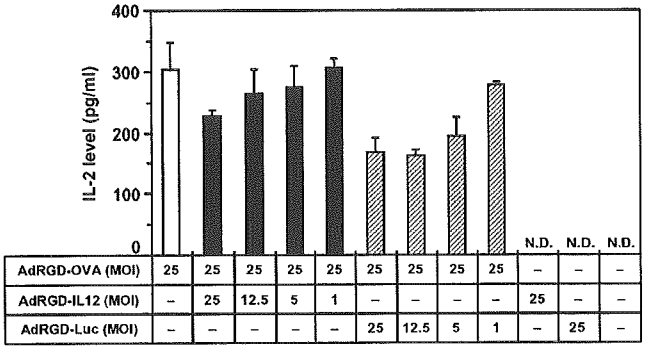

AdRGD-OVA (MOI)	25	25	25	25	25	25	25	25	25	–	–	–
AdRGD-IL12 (MOI)	–	25	12.5	5	1	–	–	–	–	25	–	–
AdRGD-Luc (MOI)	–	–	–	–	–	25	12.5	5	1	–	25	–

Figure 4 Antigen presentation on MHC class I molecules by DCs cotransduced with OVA and IL-12 gene by AdRGD. DCs were cotransduced with AdRGD-OVA and either AdRGD-IL12 or AdRGD-Luc at the indicated MOI for 2 hours. The levels of OVA peptide presentation via MHC class I molecules by transduced DCs were determined by bioassay using CD8-OVA 1.3 cells. The data represent the mean ± SD of three independent cultures. ND: IL-2 secreted from CD8-OVA 1.3 cells was not detectable.

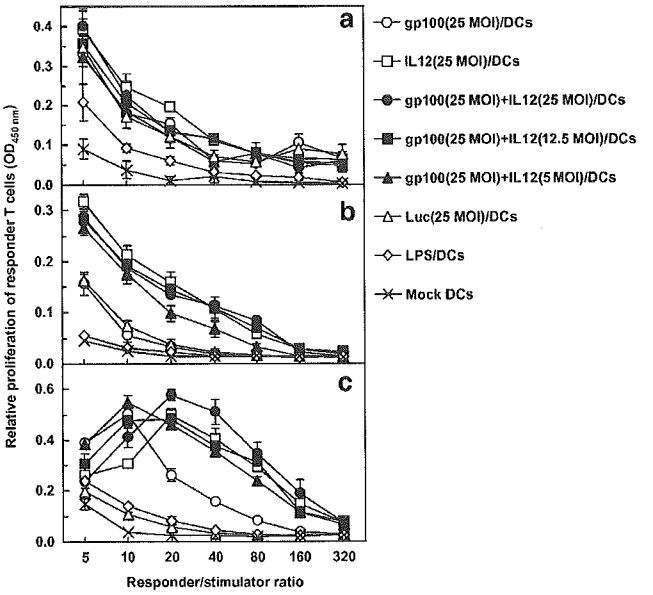

Figure 5 Allogeneic and syngeneic T-cell proliferation-stimulating ability of DCs cotransduced with gp100 and IL-12 gene by AdRGD. C57BL/6 DCs were transduced with the indicated combinations of various AdRGDs at the indicated MOI for 2 hours. Naive BALB/c T lymphocytes (**a**), naive C57BL/6 T lymphocytes (**b**), or gp100-primed C57BL/6 T lymphocytes (**c**), were cocultured with transduced, LPS-stimulated, or mock DCs at different responder/stimulator ratios for 3 days. Cell cultures were pulsed with BrdU during the last 18 hours, and then T-cell proliferation was assessed by BrdU-ELISA. Results are expressed as mean ± SE of three independent cultures using T cells prepared from three individual mice.

antigen-presentation pathway in DCs simultaneously expressing distinct proteins due to the presence of multiple AdRGDs. The variation in effects of coexpressed endogenous antigens in DCs might be induced by proteins accumulating in the cytoplasm and secreted to extracellular fluid, such as luciferase and IL-12, respectively. Taken together, antigen-presenting levels via MHC class I molecules on DCs transduced with AdRGD encoding antigen were slightly decreased by increasing dose of combined AdRGD-IL12.

T-cell-stimulating ability of DCs cotransduced with gp100 and IL-12

We performed allogeneic and syngeneic MLR to compare T-cell proliferation-stimulating ability of DCs transduced with AdRGD-gp100 alone or a combination of AdRGD-gp100 and AdRGD-IL12. DCs transduced with AdRGD-gp100 alone at 25 MOI (gp100(25MOI)/DCs), AdRGD-IL12 alone at 25 MOI (IL12(25MOI)/DCs), AdRGD-Luc alone at 25 MOI (Luc(25MOI)/DCs), or various combinations of AdRGD-gp100 and AdRGD-IL12 (gp100 (25MOI) + IL12(25MOI)/DCs, gp100(25MOI) + IL12(12.5 MOI)/DCs, and gp100(25MOI) + IL12(5MOI)/DCs) could equally stimulate proliferation of allogeneic naive T cells used as responder cells (Fig 5a). In addition, T-cell proliferation levels in these groups were higher than those not only in mock DCs but also LPS/DCs. These data indicated that DCs transduced by using AdRGD could sufficiently provide proliferative stimuli to T cells through allogeneic interaction of MHC molecules/T-cell receptors and costimulatory signals, regardless of the quantity of IL-12 secreted from DCs. On the other hand, IL12(25-MOI)/DCs, gp100(25MOI) + IL12(25MOI)/DCs, gp100 (25MOI) + IL12(12.5MOI)/DCs, and gp100(25MOI) + IL12(5MOI)/DCs could more strongly stimulate syngeneic naive T-cell proliferation as compared with gp100(25MOI)/DCs or Luc(25MOI)/DCs (Fig 5b), suggesting that *in vitro* syngeneic naive T-cell proliferation by DCs cotransduced with AdRGD-gp100 and AdRGD-IL12 was greatly influenced by secreted IL-12 rather than antigen-presentation via MHC molecules. Furthermore, in comparison with gp100(25MOI)/DCs, DCs transduced with AdRGD-IL12 alone or in combination with AdRGD-gp100 could induce considerable proliferation of syngeneic gp100-primed T cells, which were purified from C57BL/6 mice vaccinated beforehand with 10^6 gp100(25MOI)/DCs (Fig 5c). However, proliferation levels of syngeneic gp100-primed T cells stimulated by DCs transduced with AdRGD-IL12 alone or in combination with AdRGD-gp100 decreased at high responder/stimulator ratios, and this suppressive effect became remarkable at high AdRGD-IL12 MOI during gene transduction. These observations suggested that excessive IL-12 secreted from transduced DCs might inhibit proliferation or induce cell death in activated T cells.

In addition, we assessed by ELISA the Th1/Th2 cytokine balance in media of syngeneic naive T cells cocultured with various transduced DCs for 5 days at a responder/stimulator ratio of 10 in the presence of 10 U/ml recombinant murine IL-2 (Table 1). IL12(25MOI)/DCs, gp100(25MOI) + IL12(25MOI)/DCs, gp100(25MOI) + IL12(12.5MOI)/DCs, and gp100(25MOI) + IL12(5MOI)/DCs could markedly enhance Th1-skewing IFN-γ secretion from syngeneic naive T cells as compared with mock

Table 1 Cytokine secretion from syngeneic naive T cells cocultured with various transduced DCs

DC treatment				
AdRGD-gp100 (MOI)	AdRGD-IL12 (MOI)	IFN-γ (ng/ml)	IL-4 (pg/ml)	IL-10 (pg/ml)
—	—	0.25±0.05	<15	<30
25	—	1.00±0.19	<15	<30
—	25	17.17±0.48	<15	<30
25	25	25.78±1.84	<15	<30
25	12.5	18.61±1.47	<15	<30
25	5	20.23±2.96	<15	<30

Data are expressed as mean±SD of three independent cultures.

DCs, whereas only a slight increase in IFN-γ levels was observed during cocultivation with gp100(25MOI)/DCs. We confirmed that IFN-γ secretion was undetectable in control wells in which only transduced or mock DCs were cultured. On the other hand, secretion of the Th2 cytokines, IL-4 and IL-10, was not detectable in any syngeneic T cells stimulated by transduced or mock DCs. These results suggested that DCs cotransduced with gp100 and IL-12 could more efficiently differentiate sensitized T cells at the Th1-biasing state (the cellular immunity-dominant state), which is required for the induction of efficacious tumor immunity.

Vaccine efficacy of DCs cotransduced with gp100 and IL-12

In order to evaluate the potency of DCs cotransduced with gp100 and IL-12 as vaccine carriers, we investigated protective efficacy against murine B16BL6 melanoma challenge (Fig 6). C57BL/6 mice received a single intradermal injection of 2×10^5 DCs transduced with various combinations of AdRGD-gp100, AdRGD-IL12, and AdRGD-Luc, and then these mice were inoculated with 2×10^5 B16BL6 melanoma cells at 1 week post-immunization. Obvious growth suppression of the challenging B16BL6 tumor was achieved in mice vaccinated with gp100(25MOI)/DCs, as shown in our previous report,[9] whereas the mice immunized with IL12(25-MOI)/DCs or Luc(25MOI)/DCs showed little or no protective effect as compared with vehicle-injected mice. In addition, a more potent inhibitory effect on tumor growth could be observed in mice after vaccination with gp100(25MOI)+IL12(5MOI)/DCs than in mice vaccinated with gp100(25MOI)/DCs. However, vaccine efficacy of DCs cotransduced with gp100 and IL-12 tended to diminish with increasing AdRGD-IL12 MOI during gene transduction, and immunization with gp100(25MOI)+Luc(25MOI)/DCs led to inferior anti-tumor effects compared to those of the gp100(25MOI)/DCs group.

Furthermore, we investigated the cytolytic activities of NK cells and CTLs in mice intradermally immunized with DCs cotransduced with gp100 and IL-12 by Eu-release

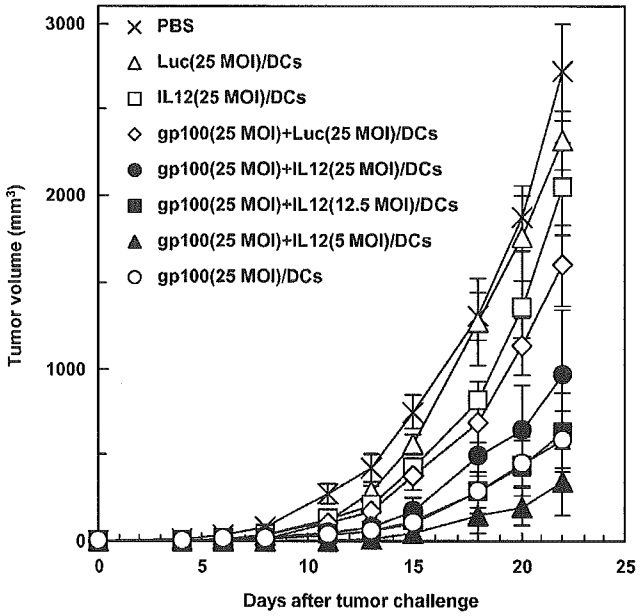

Figure 6 Vaccine efficacy of DCs cotransduced with gp100 and IL-12 gene by AdRGD against B16BL6 melanoma challenge. DCs were transduced with the indicated combinations of various AdRGDs at the indicated MOI for 2 hours. C57BL/6 mice were immunized by intradermal injection of transduced DCs into the left flank at 2×10^5 cells, and then 2×10^5 B16BL6 melanoma cells were inoculated into the right flank of the mice 1 week postvaccination. The size of tumors was assessed using microcalipers three times per week. Each point represents the mean±SE of 6–12 mice. Statistical analysis of tumor volume on day 22 after tumor challenge was carried out by Mann-Whitney *U*-test. $P<.01$ (■, ▲, ○), $P<.05$ (●), not significant (×, □, ◇) *versus* Luc(25MOI)/DCs (△). $P<.01$ (×, △, □, ◇), not significant (●, ■, ▲) *versus* gp100(25MOI)/DCs (○).

assay. At 1 week after immunization of C57BL/6 mice with various DC vaccines, the splenocytes were used in a cytolytic assay against YAC-1 and EL4 cells, and were restimulated *in vitro* with inactivated B16BL6 cells, which were treated with recombinant murine IFN-γ to promote the expression of their MHC class I molecules, for CTL expansion. As shown in Figure 7a, the splenic cytolytic activity against YAC-1 cells markedly increased after immunization with gp100(25MOI)+IL12(25MOI)/DCs as well as IL12(25MOI)/DCs, whereas EL4 cells were not injured by splenocytes prepared from any groups. Effector cells from mice immunized with gp100(25MOI)+IL12(5MOI)/DCs exhibited equivalent NK activity to those from mice immunized with gp100(25MOI)/DCs. These data indicated that the non-specific NK activity involved in the anti-B16BL6 melanoma response was enhanced with the increase in IL-12 secretion from the administered DC vaccine. On the other hand, the cytolytic effects on B16BL6 cells by *in vitro* restimulated effector cells was promoted in mice immunized with gp100(25MOI)+IL12(5MOI)/DCs as compared with mice immunized with gp100(25MOI)/DCs (Fig 7b). This cytolytic activity was caused by B16BL6-specific CTLs because the effector cells prepared from

mice immunized with IL12(25MOI)/DCs or mock DCs did not injure the B16BL6 cells and no cytolytic effects against syngeneic irrelevant EL4 cells were detected in any group. However, consistent with the protective effect against B16BL6 tumor challenge, mice vaccinated with gp100(25MOI) + IL12(25MOI)/DCs showed lower B16BL6-specific CTL activity than mice immunized with gp100(25MOI)/DCs.

Therefore, immunization with DCs genetically modified to express simultaneously gp100 and IL-12 exhibited duplicity for the host's immune response in our experimental model. That is, as compared with DCs transduced with AdRGD-gp100 alone, DCs cotransduced with AdRGD-IL12 at a relatively low ratio to AdRGD-gp100 were equal in inducibility of NK activity, but could more efficiently induce anti-B16BL6 tumor effects and antigen-specific CTL activity. In contrast, DCs combined with a high dose of AdRGD-IL12 during gene transduction could enhance NK activity, but attenuated B16BL6-protective efficacy and CTL activity.

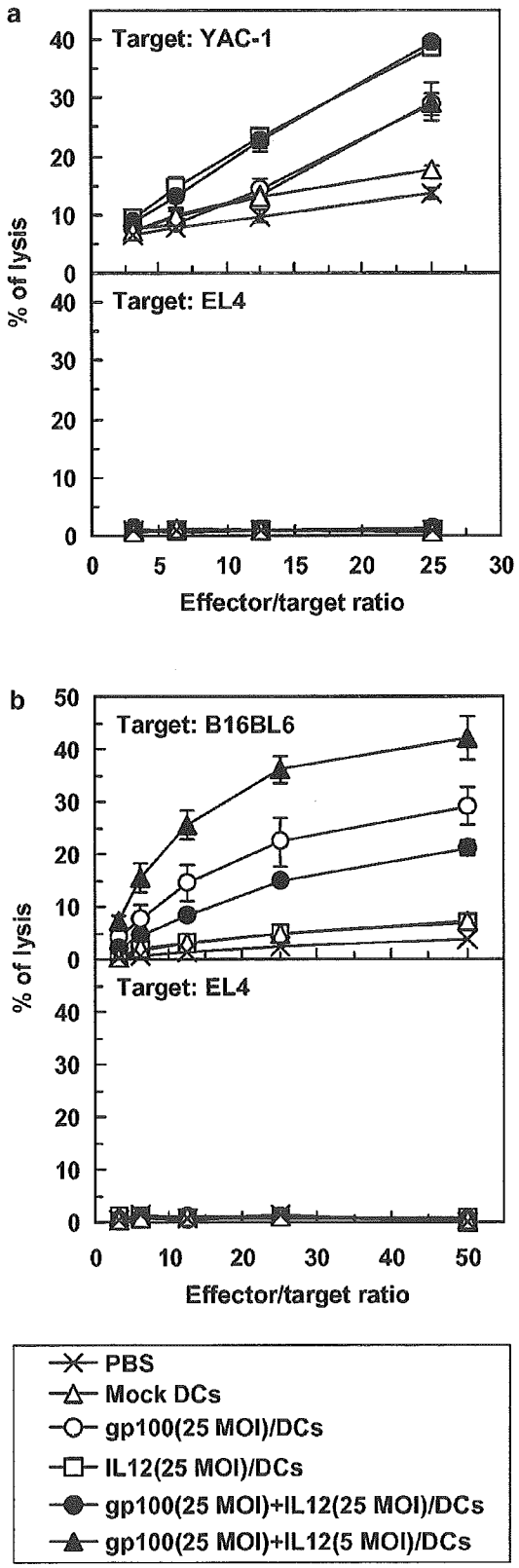

Discussion

Since DCs are the most potent APCs and are uniquely capable of presenting novel antigens to naive T cells to initiate and modulate immune responses,[1,2] various DC-based vaccines for use in immune intervention strategies against cancer have been designed and studied in many research organizations. Antitumor CTLs play a central role in the tumor-specific immune response, and the efficient priming and subsequent activation of antitumor CTLs requires the processing and presentation of TAAs as peptide fragments in the context of appropriate MHC class I molecules by APCs.[31] In addition, a Th1-biased cytokine balance is desirable for sensitization of CTLs specific for TAA by APCs. IL-12 is the key factor that skews the immune balance toward a Th1 response and that can promote a switch from an established Th2 to a Th1 response.[32,33] In fact, potent antitumor effects of DCs genetically engineered with IL-12 have been demonstrated in several murine models by vaccination using TAA-derived peptide pulsed DCs or intratumoral injection using unpulsed DCs.[34–36] Therefore, we believe that, as compared with DCs delivered with TAA gene alone, DCs genetically manipulated to express simultaneously TAA and IL-12 might be a promising vaccine carrier

Figure 7 NK (**a**) and B16BL6-specific CTL (**b**) activity in mice immunized with DCs cotransduced with gp100 and IL-12 gene by AdRGD. DCs were transduced with the indicated combinations of AdRGD-gp100 and AdRGD-IL12 at the indicated MOI for 2 hours. Transduced or mock DCs were vaccinated once intradermally into C57BL/6 mice at 2×10^5 cells. At 1 week after immunization, nonadherent splenocytes were prepared from these mice, and directly used in cytolytic assays against YAC-1 and EL-4 cells (**a**). In addition, the isolated splenocytes were restimulated *in vitro* for 5 days with IFN-γ-stimulated and MMC-inactivated B16BL6 cells. A cytolytic assay using the restimulated splenocytes was performed against IFN-γ-stimulated B16BL6 and EL4 cells (**b**). Each point represents the mean $\pm$ SE of four independent cultures from four individual mice.

capable of generating more efficacious antitumor responses because of their ability to induce Th1-polarized responses.

A vector system, which can effectively deliver a foreign gene to DCs, is required to create a genetically modified DC vaccine having a potential to improve the efficacy of DC-based immunotherapy. We have demonstrated that AdRGD enabled highly efficient gene transduction into murine and human DCs because of the targeting of αv-integrin by the RGD sequence inserted at the HI-loop in their fiber knob.[6–9] When mouse bone marrow-derived DCs were cotransduced with AdRGD-gp100 and AdRGD-IL12, their expression of gp100 and IL-12 was comparable to that in DCs transduced with each AdRGD alone (Figs 1 and 2). IL-12 secreted from these DCs is biologically active because direct intratumoral injection of AdRGD-IL12, used in the present study and whose expression cassette was designed to be transcribed from IL-12p35 cDNA to the internal ribosome entry site sequence to IL-12p40 cDNA under the control of the cytomegalovirus promoter, could induce tumor regression based on promotion of tumor immunity in melanoma-bearing mice.[37] RT-PCR analysis (Fig 1) suggested that LPS-driven maturation or irrelevant AdRGD transduction could moderately enhance expression of the IL-12p40 subunit mRNA in DCs, but not IL-12p35 subunit mRNA. Several reports have demonstrated that the production of the two IL-12 subunits is regulated by different mechanisms, mainly at the level of mRNA expression, and that the level of bioactive IL-12p70 production in APCs in response to LPS and cytokines is determined by the level of IL-12p35 expression.[38,39] Therefore, DCs cannot attain sufficient IL-12p70 productivity, which is based on enhancement of endogenous gene expression of the two subunits, via a maturation signal from LPS or AdRGD transduction alone. Taken together, our results demonstrated that DCs cotransduced with AdRGD-gp100 and AdRGD-IL12 could simultaneously express gp100 and IL-12 at levels equal to DCs transduced with each vector alone, indicating that DCs can obtain several additional functions by using a combination of AdRGDs carrying different genes.

Full analysis and understanding of immunological characteristics of DC vaccine are imperative for the development of DC-based immunotherapy because the polarity of the immune response is greatly influenced by the activated state of DCs during T-cell sensitization. Flow cytometric analysis indicated that the expression of MHC class I/II, CD40, CD80, and CD86 molecules was enhanced only by AdRGD-transduction, and that DCs transduced with the IL-12 gene exhibited considerable upregulation of MHC class I, CD40, and CD86 molecules on their surface in response to autocrine effects of secreted IL-12 as compared with DCs transduced with AdRGD-gp100 alone (Fig 3). On the other hand, DCs cotransduced with OVA and IL-12 by AdRGDs exhibited lower OVA-presentation levels via MHC class I molecules than DCs transduced with AdRGD-OVA alone (Fig 4), although the cytoplasmic expression of endogenous antigen introduced into DCs was not affected by the combination with other AdRGDs (Fig 2a). In addition, OVA-presentation levels in DCs transduced with AdRGD-OVA were markedly decreased by combination with AdRGD-Luc, which expresses luciferase as another endogenous antigen (Fig 4). These inconsistent results suggested that processing machineries in the MHC class I-presentation pathway may compete with multiple proteins transduced by the combination of AdRGDs, and that localization characteristics, such as cytoplasmic accumulation, extracellular secretion, and plasma membrane-specific localization, of other proteins should be considered during the preparation of DCs expressing TAA and other functional proteins by cotransduction with multiple AdRGDs in an attempt to maintain sufficient TAA-presenting capacity. With regard to T-cell-stimulating ability, DCs cotransduced with gp100 and IL-12 could more effectively enhance proliferation of syngeneic naive and gp100-primed T cells than DCs transduced with gp100 alone, although allogeneic T-cell proliferation did not differ between the two types of transduced DCs (Fig 5). Furthermore, we could detect considerable IFN-γ secretion from syngeneic naive T cells stimulated by DCs cotransduced with gp100 and IL-12 (Table 1), as expected. These data from *in vitro* immunological analysis suggested that DCs cotransduced with TAA and IL-12 using AdRGD can function as useful vaccine carriers possessing TAA-presentation ability, sufficient T-cell-stimulating ability, and Th1-driving ability *in vivo*.

We attempted to compare vaccine efficacy of DCs genetically modified with various combinations of AdRGD-gp100, AdRGD-IL12, and AdRGD-Luc using the murine B16BL6 melanoma model. Although mice vaccinated with gp100(25MOI) + IL12(5MOI)/DCs exhibited more effective suppression of B16BL6 tumor growth and efficient induction of B16BL6-specific CTLs than those vaccinated with gp100(25MOI)/DCs, vaccine efficacy of cotransduced DCs diminished with increasing combined AdRGD-IL12 MOI during gene transduction, contrary to our expectation (Figs 6 and 7). We speculated that this adverse effect might be caused by a decrease in antigen presentation in DCs by coexpression of TAA and IL-12 as shown in Figure 4, because the anti-B16BL6 effect of gp100(25MOI) + Luc(25MOI)/DCs was obviously inferior to that by gp100(25MOI)/DCs. An alternative explanation for the negative effect of AdRGD-IL12-cotransduction includes an immunosuppressive effect of excess IL-12 on the host's immune cells. Several studies have demonstrated that IL-12 inhibits cell-mediated immune responses, such as clonal expansion of CTLs, in a dose-dependent manner through IFN-γ-mediated nitric oxide production by macrophages in the murine models.[40–43] The *in vivo* bimodal effect of DCs cotransduced with gp100 and IL-12 in our model might involve immunosuppression based on nitric oxide, because DCs transduced with AdRGD-IL12 could drastically enhance IFN-γ secretion from syngeneic naive T cells in MLR (Table 1). In addition, Piccioli et al[44] reported that an *in vitro* interaction between activated NK cells and DCs at high NK/DC ratios resulted in inhibition of DC functions due to potent killing by NK cells,

whereas this interaction at low NK/DC ratios led to drastic increases in DC cytokine production. Therefore, a remarkable increase in NK activity in mice that were vaccinated with gp100(25MOI) + IL12(25MOI)/DCs, as shown in Figure 7, might suppress the induction of the B16BL6-specific immune response by the administered DC vaccine.

To date, vaccine efficacy of DCs cotransduced with TAA and IL-12 has not been fully clarified because both positive[45] and negative[46] effects of simultaneous expression of IL-12 in DC vaccine have been reported. Based on the results of the present study, we concluded that determination of the specific vector dose capable of optimizing both TAA-presentation levels and IL-12-secretion levels in DC vaccine is essential for improving antitumor efficacy based on active biasing of the immune response toward a cellular immunity dominated state.

Abbreviations

2-ME, 2-mercaptoethanol; AdRGD, RGD fiber-mutant adenovirus vector; APC, antigen-presenting cell; BrdU, 5-bromo-2′-deoxyuridine; CTL, cytotoxic T lymphocyte; DC, dendritic cell; Eu, europium; FBS, fetal bovine serum; GM-CSF, granulocyte/macrophage colony-stimulating factor; IFN, interferon; IL, interleukin; LPS, lipopolysaccharide; mAb, monoclonal antibody; MHC, major histocompatibility complex; MLR, mixed leukocyte reaction; MMC, mitomycin C; MOI, multiplicity of infection; NK, natural killer; OVA, ovalbumin; PBS, phosphate-buffered saline; RT-PCR, reverse transcription-polymerase chain reaction; TAA, tumor-associated antigen; Th, helper T cell.

Acknowledgments

We are grateful to Dr Hiroshi Yamamoto (Department of Immunology, Graduate School of Pharmaceutical Sciences, Osaka University, Suita, Japan) for providing mIL12 BIA/pBluescript II KS(-), to Dr Hirofumi Hamada (Department of Molecular Medicine, Sapporo Medical University, Sapporo, Japan) for providing pAx1-CA h-gp100, to Dr Michael J Bevan (Department of Immunology, Howard Hughes Medical Institute, University of Washington, Seattle, WA) for providing pAc-neo-OVA, to Dr Clifford V Harding (Department of Pathology, Case Western Reserve University, Cleveland, OH) for providing CD8-OVA 1.3 cells, to Yasushige Masunaga, Masaya Nishida, and Aya Matsui (Department of Biopharmaceutics, Kyoto Pharmaceutical University, Kyoto, Japan) for technical assistance, and to KIRIN Brewery Co., Ltd (Tokyo, Japan) for providing recombinant murine GM-CSF.

The present study was supported in part by the Research on Health Sciences focusing on Drug Innovation from The Japan Health Sciences Foundation; by the Science Research Promotion Fund of the Japan Private School Promotion Foundation; by grants from the Bioventure Development Program of the Ministry of Education, Culture, Sports, Science and Technology of Japan; and by grants from the Ministry of Health, Labour and Welfare in Japan.

References

1. Banchereau J, Steinman RM. Dendritic cells and the control of immunity. *Nature*. 1998;392:245–252.
2. Kapsenberg ML. Dendritic-cell control of pathogen-driven T-cell polarization. *Nat Rev Immunol*. 2003;3:984–993.
3. Nestle FO, Alijagic S, Gilliet M, et al. Vaccination of melanoma patients with peptide- or tumor lysate-pulsed dendritic cells. *Nat Med*. 1998;4:328–332.
4. Thurner B, Haendle I, Roder C, et al. Vaccination with mage-3A1 peptide-pulsed mature, monocyte-derived dendritic cells expands specific cytotoxic T cells and induces regression of some metastases in advanced stage IV melanoma. *J Exp Med*. 1999;190:1669–1678.
5. Yu JS, Wheeler CJ, Zeltzer PM, et al. Vaccination of malignant glioma patients with peptide-pulsed dendritic cells elicits systemic cytotoxicity and intracranial T-cell infiltration. *Cancer Res*. 2001;61:842–847.
6. Okada N, Tsukada Y, Nakagawa S, et al. Efficient gene delivery into dendritic cells by fiber-mutant adenovirus vectors. *Biochem Biophys Res Commun*. 2001;282:173–179.
7. Okada N, Masunaga Y, Okada Y, et al. Gene transduction efficiency and maturation status in mouse bone marrow-derived dendritic cells infected with conventional or RGD fiber-mutant adenovirus vectors. *Cancer Gene Ther*. 2003;10:421–431.
8. Okada N, Saito T, Masunaga Y, et al. Efficient antigen gene transduction using Arg-Gly-Asp fiber-mutant adenovirus vectors can potentiate antitumor vaccine efficacy and maturation of murine dendritic cells. *Cancer Res*. 2001;61:7913–7919.
9. Okada N, Masunaga Y, Okada Y, et al. Dendritic cells transduced with gp100 gene by RGD fiber-mutant adenovirus vectors are highly efficacious in generating anti-B16BL6 melanoma immunity in mice. *Gene Therapy*. 2003;10:1891–1902.
10. Hammerling GJ, Klar D, Pulm W, et al. The influence of major histocompatibility complex class I antigens on tumor growth and metastasis. *Biochim Biophys Acta*. 1987; 907:245–259.
11. Moller P, Hammerling GJ. The role of surface HLA-A,B,C molecules in tumour immunity. *Cancer Surv*. 1992;13: 101–127.
12. Khanna R. Tumour surveillance: missing peptides and MHC molecules. *Immunol Cell Biol*. 1998;76:20–26.
13. Nishimura T, Nakui M, Sato M, et al. The critical role of Th1-dominant immunity in tumor immunology. *Cancer Chemother Pharmacol*. 2000;46(Suppl):S52–S61.
14. Gubler U, Chua AO, Schoenhaut DS, et al. Coexpression of two distinct genes is required to generate secreted bioactive cytotoxic lymphocyte maturation factor. *Proc Natl Acad Sci USA*. 1991;88:4143–4147.
15. Wolf SF, Temple PA, Kobayashi M, et al. Cloning of cDNA for natural killer cell stimulatory factor, a heterodimeric cytokine with multiple biologic effects on T and natural killer cells. *J Immunol*. 1991;146:3074–3081.
16. Robertson MJ, Soiffer RJ, Wolf SF, et al. Response of human natural killer (NK) cells to NK cell stimulatory

factor (NKSF): cytolytic activity and proliferation of NK cells are differentially regulated by NKSF. *J Exp Med.* 1992;175:779–788.
17. Brunda MJ. Interleukin-12. *J Leukoc Biol.* 1994;55:280–288.
18. Chan SH, Perussia B, Gupta JW, et al. Induction of interferon gamma production by natural killer cell stimulatory factor: characterization of the responder cells and synergy with other inducers. *J Exp Med.* 1991;173: 869–879.
19. Chan SH, Kobayashi M, Santoli D, et al. Mechanisms of IFN-γ induction by natural killer cell stimulatory factor (NKSF/IL-12). Role of transcription and mRNA stability in the synergistic interaction between NKSF and IL-2. *J Immunol.* 1992;148:92–98.
20. Hsieh CS, Macatonia SE, Tripp CS, et al. Development of TH1 $CD4^+$ T cells through IL-12 produced by Listeria-induced macrophages. *Science.* 1993;260:547–549.
21. Seder RA, Gazzinelli R, Sher A, et al. Interleukin 12 acts directly on $CD4^+$ T cells to enhance priming for interferon γ production and diminishes interleukin 4 inhibition of such priming. *Proc Natl Acad Sci USA.* 1993;90: 10188–10192.
22. Nastala CL, Edington HD, McKinney TG, et al. Recombinant IL-12 administration induces tumor regression in association with IFN-γ production. *J Immunol.* 1994; 153:1697–1706.
23. Voest EE, Kenyon BM, O'Reilly MS, et al. Inhibition of angiogenesis *in vivo* by interleukin 12. *J Natl Cancer Inst.* 1995;87:581–586.
24. Pfeifer JD, Wick MJ, Roberts RL, et al. Phagocytic processing of bacterial antigens for class I MHC presentation to T cells. *Nature.* 1993;361:359–362.
25. Mizuguchi H, Koizumi N, Hosono T, et al. A simplified system for constructing recombinant adenoviral vectors containing heterologous peptides in the HI loop of their fiber knob. *Gene Therapy.* 2001;8:730–735.
26. Okada Y, Okada N, Nakagawa S, et al. Fiber-mutant technique can augment gene transduction efficacy and antitumor effects against established murine melanoma by cytokine-gene therapy using adenovirus vectors. *Cancer Lett.* 2002;177:57–63.
27. Mizuguchi H, Kay MA. Efficient construction of a recombinant adenovirus vector by an improved *in vitro* ligation method. *Hum Gene Ther.* 1998;9:2577–2583.
28. Mizuguchi H, Kay MA. A simple method for constructing E1- and E1/E4-deleted recombinant adenoviral vectors. *Hum Gene Ther.* 1999;10:2013–2017.
29. Lutz MB, Kukutsch N, Ogilvie AL, et al. An advanced culture method for generating large quantities of highly pure dendritic cells from mouse bone marrow. *J Immunol Methods.* 1999;223:77–92.
30. Okada N, Tsujino M, Hagiwara Y, et al. Administration route-dependent vaccine efficiency of murine dendritic cells pulsed with antigens. *Br J Cancer.* 2001;84:1564–1570.
31. Lanzavecchia A. Identifying strategies for immune intervention. *Science.* 1993;260:937–944.
32. Scott P, Trinchieri G. IL-12 as an adjuvant for cell-mediated immunity. *Semin Immunol.* 1997;9:285–291.
33. Shurin MR, Esche C, Peron JM, et al. Antitumor activities of IL-12 and mechanisms of action. *Chem Immunol.* 1997;68:153–174.
34. Zitvogel L, Couderc B, Mayordomo JI, et al. IL-12-engineered dendritic cells serve as effective tumor vaccine adjuvants *in vivo*. *Ann NY Acad Sci.* 1996;795:284–293.
35. Nishioka Y, Hirao M, Robbins PD, et al. Induction of systemic and therapeutic antitumor immunity using intratumoral injection of dendritic cells genetically modified to express interleukin 12. *Cancer Res.* 1999;59:4035–4041.
36. Melero I, Duarte M, Ruiz J, et al. Intratumoral injection of bone-marrow derived dendritic cells engineered to produce interleukin-12 induces complete regression of established murine transplantable colon adenocarcinomas. *Gene Therapy.* 1999;6:1779–1784.
37. Okada Y, Okada N, Mizuguchi H, et al. Optimization of antitumor efficacy and safety of *in vivo* cytokine gene therapy using RGD fiber-mutant adenovirus vector for preexisting murine melanoma. *Biochim Biophys Acta.* 2004;1670:172–180.
38. Snijders A, Hilkens CM, van der Pouw Kraan TC, et al. Regulation of bioactive IL-12 production in lipopolysaccharide-stimulated human monocytes is determined by the expression of the p35 subunit. *J Immunol.* 1996;156:1207–1212.
39. Kalinski P, Vieira PL, Schuitemaker JH, et al. Prostaglandin E_2 is a selective inducer of interleukin-12 p40 (IL-12p40) production and an inhibitor of bioactive IL-12p70 heterodimer. *Blood.* 2001;97:3466–3469.
40. Koblish HK, Hunter CA, Wysocka M, et al. Immune suppression by recombinant interleukin (rIL)-12 involves interferon gamma induction of nitric oxide synthase 2 (iNOS) activity: inhibitors of NO generation reveal the extent of rIL-12 vaccine adjuvant effect. *J Exp Med.* 1998;188:1603–1610.
41. Medot-Pirenne M, Heilman MJ, Saxena M, et al. Augmentation of an antitumor CTL response *in vivo* by inhibition of suppressor macrophage nitric oxide. *J Immunol.* 1999;163:5877–5882.
42. Lasarte JJ, Corrales FJ, Casares N, et al. Different doses of adenoviral vector expressing IL-12 enhance or depress the immune response to a coadministered antigen: the role of nitric oxide. *J Immunol.* 1999;162:5270–5277.
43. Nishioka Y, Wen H, Mitani K, et al. Differential effects of IL-12 on the generation of alloreactive CTL mediated by murine and human dendritic cells: a critical role for nitric oxide. *J Leukoc Biol.* 2003;73:621–629.
44. Piccioli D, Sbrana S, Melandri E, et al. Contact-dependent stimulation and inhibition of dendritic cells by natural killer cells. *J Exp Med.* 2002;195:335–341.
45. Chen Y, Emtage P, Zhu Q, et al. Induction of ErbB-2/neu-specific protective and therapeutic antitumor immunity using genetically modified dendritic cells: enhanced efficacy by cotransduction of gene encoding IL-12. *Gene Therapy.* 2001;8:316–323.
46. Ribas A, Amarnani SN, Buga GM, et al. Immunosuppressive effects of interleukin-12 coexpression in melanoma antigen gene-modified dendritic cell vaccines. *Cancer Gene Ther.* 2002;9:875–883.

Available online at www.sciencedirect.com
SCIENCE DIRECT®
Biochemical and Biophysical Research Communications 326 (2005) 402–409
BBRC
www.elsevier.com/locate/ybbrc

Constitutively active PDX1 induced efficient insulin production in adult murine liver

Junta Imai[a,b], Hideki Katagiri[b,*], Tetsuya Yamada[a], Yasushi Ishigaki[a], Takehide Ogihara[b], Kenji Uno[a,b], Yutaka Hasegawa[a,b], Junhong Gao[a,b], Hisamitsu Ishihara[a], Hironobu Sasano[c], Hiroyuki Mizuguchi[d], Tomoichiro Asano[e], Yoshitomo Oka[a]

[a] *Division of Molecular Metabolism and Diabetes, Tohoku University Graduate School of Medicine, Japan*
[b] *Division of Advanced Therapeutics for Metabolic Diseases, Center for Translational and Advanced Animal Research, Tohoku University Graduate School of Medicine, Japan*
[c] *Division of Anatomic Pathology, Tohoku University Graduate School of Medicine, Sendai 980-8575, Japan*
[d] *Division of Cellular and Gene Therapy Products, National Institute of Health Science, Tokyo, Japan*
[e] *Department of Physiological Chemistry and Metabolism, University of Tokyo, Tokyo 113-8655, Japan*

Received 21 October 2004
Available online 19 November 2004

Abstract

To generate insulin-producing cells in the liver, recombinant adenovirus containing a constitutively active mutant of PDX1 (PDX1-VP16), designed to activate target genes without the need for protein partners, was prepared and administered intravenously to streptozotocin (STZ)-treated diabetic mice. The effects were compared with those of administering wild-type PDX1 (wt-PDX1) adenovirus. Administration of these adenoviruses at 2×10^8 pfu induced similar levels of PDX1 protein expression in the liver. While wt-PDX1 expression exerted small effects on blood glucose levels, treatment with PDX1-VP16 adenovirus efficiently induced insulin production in hepatocytes, resulting in reversal of STZ-induced hyperglycemia. The effects were sustained through day 40 when exogenous PDX1-VP16 protein expression was undetectable in the liver. Endogenous PDX1 protein came to be expressed in the liver, which is likely to be the mechanism underlying the sustained effects. On the other hand, albumin and transferrin expressions were observed in insulin-producing cells in the liver, suggesting preservation of hepatocytic functions. Thus, transient expression of an active mutant of PDX1 in the liver induced sustained PDX1 and insulin expressions without loss of hepatocytic function.

Keywords: Insulin; PDX1; Gene therapy; Diabetes; Adenovirus; Transdifferentiation

Type 1 diabetes mellitus is characterized by progressive loss of pancreatic β cells, leading to a lifelong dependency on insulin treatments. Recently, marked advances have been made in transplanting pancreatic islets from human cadavers into type 1 diabetics [1]. However, immune rejection and donor supply are still major challenges in islet cell transplantation. In this context, generation of insulin-producing cells by somatic gene therapy may represent a viable alternative for the treatment for diabetes.

The liver is a possible target organ for generation of insulin-producing cells. Pancreatic and hepatic tissues both express several transcription factors such as HNF1α and C/EBPβ. In addition, these tissues also have similar glucose sensing machinery consisting of the GLUT2 glucose transporter and glucokinase. Furthermore, during embryogenesis, the liver and the ventral pancreas appear to arise from the same cell

* Corresponding author. Fax: +81 22 717 8228.
E-mail address: katagiri-tky@umin.ac.jp (H. Katagiri).

0006-291X/$ - see front matter © 2004 Elsevier Inc. All rights reserved.
doi:10.1016/j.bbrc.2004.11.047

population located within the embryonic endoderm [2]. The gene most likely to be responsible for the difference between the liver and pancreas is pancreatic and duodenal homeobox gene 1 (PDX1), also known as IDX1/IPF1/STF1. PDX1 is expressed in pancreatic buds in the endoderm prior to morphological development of the pancreas [3,4] and has been shown to play a fundamental role in regulating pancreatic development. Gene disruption of PDX1 has been shown to inhibit pancreatic bud maturation and outgrowth, resulting in complete absence of the pancreas [5]. In addition, conditional inactivation of PDX1 in insulin-producing cells results in a progressive loss of β cells, suggesting PDX1 to play an essential role in maintaining β cells [6].

Therefore, to generate insulin-producing cells, several groups have overexpressed PDX1 in various sites [7–11]. Adenovirus-mediated transfer of the PDX1 gene reportedly ameliorates streptozotocin (STZ)-induced hyperglycemia in a short time (within 10 days) [7] as well as for longer periods [12] via production of insulin in the liver. However, helper-dependent adenovirus (HDAD)-mediated PDX1 gene transfer into the liver reportedly results in severe hepatitis and functional failure due to production of pancreatic exocrine enzymes [10]. In addition, transgenic mice overexpressing PDX1 in the liver also develop liver failure [11].

PDX1 has been shown to activate target genes by association with several co-factors such as PBX [13] and the expressions of these protein partners are absent in the liver. To produce a version of PDX1 that would activate target genes without the need for protein partners, the VP16 activation domain from herpes simplex virus was fused to the C-terminus of PDX1 (PDX1-VP16). In PDX1-VP16 transgenic *Xenopus* tadpoles, part or all of the liver is converted to pancreatic tissue, while hepatic differentiation products are lost from the regions converted to pancreas [14].

Therefore, in the present study, we prepared PDX1-VP16 adenovirus and compared the effects of PDX1-VP16 expression with those of wt-PDX1 in the adult murine liver in vivo. These recombinant adenoviruses were administered at a titer of 2×10^8 pfu, which is one to two orders of magnitude lower than those used in previous reports [7,12]. Herein we demonstrate PDX1-VP16 gene transduction to induce hepatocytic production of insulin, but not glucagon or amylase, more efficiently than wt-PDX1, resulting in reversal of STZ-induced hyperglycemia. We found that PDX1-VP16 gene therapy induced endogenous PDX1 expression in the liver, and hence sustained expression of insulin. In contrast to transgenic tadpole experiments, the conversion was partial and liver-specific gene expressions including those of albumin and transferrin were maintained in insulin-producing cells.

Materials and methods

Recombinant adenoviruses. Murine PDX1 cDNA was cloned from a MIN6 cDNA library by PCR. Using PCR, the *Cla*I site was added to murine PDX1 cDNA, which was digested with *Cla*I and subcloned into VP16-N (kind gift from Dr. H. Kanamori) as described [14]. Recombinant adenoviruses containing wt-PDX1 and PDX1-VP16 cDNA were prepared as reported previously [15–17]. LacZ adenovirus was used as a control [18].

Animals. Male C57BL/6N mice were purchased from Clea (Tokyo, Japan), housed in an air-conditioned environment, with a 12-h light-dark cycle, and fed a regular unrestricted diet. Diabetes was induced by intraperitoneal injection of 160–170 mg/kg STZ (Sigma St. Louis, MO) in citrate buffer at 5–6 weeks of age. Blood glucose was determined after a 10 h fast at 6 days after STZ injection; mice with fasting glucose levels of 300–600 mg/dl were used for the experiments. The mice were treated with 2×10^8 plaque-forming units of recombinant adenovirus by systemic injection into the tail vein and killed 40 days after adenovirus injection. Serum insulin concentrations were measured using a rat insulin ELISA Kit Ultra Sensitive (Morinaga, Tokyo, Japan).

Oral glucose tolerance tests. Oral glucose tolerance tests were performed 40 days after adenovirus infusion. Serum glucose levels were determined before, and 15, 30, 60, 90, and 120 min after, administration of oral glucose (1 g/kg body weight).

Immunoblotting. Liver samples were homogenized in buffer (100 mM Tris, pH 8.5, 250 mM NaCl, 1% BP-40, and 1 mM EDTA). Tissue homogenates were centrifuged at 14,000*g* for 10 min at 4 °C. Supernatants including tissue protein extracts (180 μg total protein) were then boiled in Laemmli buffer containing 10 mM dithiothreitol. Aliquots of proteins (15 μg) were subjected to SDS–PAGE. Immunoblot analyses were performed using ECL plus a Western Blotting Detection System Kit (Amersham Buckinghamshire, UK). Antibodies to PDX1 (A-17, Santa Cruz Biotechnology, Santa Cruz, CA) and HSV-1 VP16 (vA-19, Santa Cruz Biotechnology) were commercially obtained.

Immunohistochemistry. Livers of mice were excised 40 days after adenoviral treatment and fixed overnight in 10% paraformaldehyde. Fixed tissues were processed for paraffin embedding and 3 μm sections were prepared. For immunohistochemistry, the streptavidin–biotin (SAB) method was performed using a Histofine SAB-PO kit (Nichirei, Tokyo, Japan) for insulin, glucagon, and amylase, and a MAX-PO kit (Nichirei) for somatostatin, and an EnVision kit/HRP (DAKO, Glostrup, Denmark) for pancreatic polypeptide. Slides were deparaffinized, and then were either autoclaved in citrate buffer for antigen retrieval before being incubated in blocking solution (for amylase, somatostatin, and pancreatic polypeptide detection), or immediately exposed to the blocking solution (for insulin and glucagon detection). For insulin detection, sections were incubated for 18 h at 4 °C with monoclonal antibody against human insulin (Sigma) diluted 1:1000 in PBS. For detection of glucagon, sections were incubated for 18 h at 4 °C with antiserum raised against human glucagon (DAKO) diluted 1:3000 in PBS. For detection of somatostatin, sections were incubated overnight at 4 °C with rat anti-somatostatin monoclonal antibody (Chemicon, Temecula, CA) diluted 1:100 in PBS. For detection of pancreatic polypeptide, sections were incubated overnight at 4 °C with antiserum raised against rat pancreatic polypeptide (LINCO, St. Charles, MO) diluted 1:100 in PBS. For detection of amylase, sections were incubated for 18 h at 4 °C with antiserum raised against the C-terminus of human amylase (Santa Cruz Biotechnology) diluted 1:1000 in PBS. Slides were then incubated with the biotinylated IgG for 1 h and next with peroxidase-conjugated streptavidin for 30 min at room temperature. Finally, immunoreactivity was visualized by incubation with a substrate solution containing 3,3′-diaminobenzidine tetrahydrochloride (DAB).

Fluorescent immunocytochemistry. The 3 μm sections of paraffin-embedded liver were processed as follows. For double staining of

insulin and transferrin or albumin, the sections were incubated overnight with antibodies against insulin and transferrin (goat polyclonal; Santa Cruz Biotechnology) or albumin (rabbit polyclonal; Biogenesis, Kingston, New Hampshire) at 4 °C. Antibodies against insulin, transferrin, and albumin were diluted 1:1000, 1:5000, and 1:5000, respectively, in PBS. For double staining of insulin and transferrin, the sections were then incubated for 1 h at room temperature in a mixture of TRITC-conjugated sheep anti-mouse IgG and FITC-conjugated donkey anti-goat IgG (Jackson Immuno Research, West Grove, PA) diluted 1:1000 in PBS. For double staining of insulin and albumin, the sections were incubated in a mixture of Alexa Fluor 488 goat anti-mose IgG (Molecular Probes, Eugene, OR) and Alexa Fluor 546 goat anti-rabbit IgG diluted 1:1000 in PBS. Sections were observed under a fluorescence microscope (Leica DM RXA, Leica Microsystems, Wetzlar, Germany). The image was analyzed with a Q-fluoro analyzing system (Leica).

Results

To express a PDX1 mutant, in the liver, which is constitutively active without association with protein partners, we prepared a recombinant adenovirus encoding the VP16 activation domain from herpes simplex virus [19,20] fused to the C-terminus of murine PDX1 (PDX1-VP16). For comparison, we also prepared recombinant adenoviruses encoding the wild-type PDX1 (wt-PDX1) and LacZ. These recombinant adenoviruses, at 2×10^8 pfu, were injected intravenously 6 days after STZ administration, when hyperglycemia had already developed; blood glucose levels after a 10 h fast were approximately 400 mg/dl (Fig. 1B). Mice given the LacZ adenovirus were used as controls (LacZ-mice). Systemic infusion of recombinant adenoviruses into mice through the tail vein caused transgene expression primarily in the liver, with no detectable expression in peripheral tissues such as muscle, fat, kidney or brain (data not shown), as reported previously [21].

As shown in Fig. 1A, immunoblotting of hepatic lysates on day 3 after adenoviral administration with anti-PDX1 antibody revealed that ectopic expression of wt-PDX1 or PDX1-VP16 was obtained in the liver. Administration of recombinant adenoviruses at the same titer induced similar levels of PDX1 protein expression.

We next examined the effects of treatment with these adenoviruses on STZ-induced hyperglycemia (Fig. 1B). Administration of wt-PDX1 adenovirus did not significantly decrease fasting blood glucose levels through day 20. Although, interestingly, fasting blood glucose levels were slightly but significantly decreased after day 30 as compared with those in STZ-treated LacZ-mice, administration of wt-PDX1 adenovirus at such a low titer exerted only very small effects in terms of reversal of hyperglycemia.

In contrast, administration of PDX1-VP16 adenovirus more effectively reversed STZ-induced hyperglycemia (Fig. 1B). Hepatic expression of PDX1-VP16 induced significant, profound decreases in fasting blood glucose levels. Although fasting blood glucose levels rose slightly between day 10 and day 15, the therapeutic effects were sustained throughout the experiments. As shown in Table 1, some variation in results was observed. Thirteen percent of PDX1-VP16-mice exhibited almost no decrease in blood glucose levels, although the proportion of these mice was significantly lower than that of wt-PDX1-mice. In contrast, in 27% of PDX1-VP16-mice, fasting blood glucose levels were lower than 200 mg/dl. No such normalization of glucose levels was obtained by wt-PDX1 adenovirus administration (Table 1). Thus, PDX1-VP16 expression in the liver more effectively lowered blood glucose levels and these effects persisted even after adenoviral-mediated gene expression had declined.

To examine the mechanism whereby administration of PDX1-VP16 adenovirus efficiently and persistently lowered blood glucose levels in STZ-treated mice, liver sections from these mice on day 40 after adenoviral administration were immunostained with anti-insulin antibody (Fig. 1C). No insulin staining was detectable in the livers of LacZ-mice. In wt-PDX1-mice, very faint staining with anti-insulin antibody was detected in the liver. In contrast, in PDX1-VP16 mice, strong insulin staining was detected in the cytoplasm of hepatocytes in scattered portions of the liver. The insulin positive cells were seen mostly around vessels. The scant residual insulin-positive cells in the pancreas did not differ significantly among these mice (data not shown). Thus, insulin secretion from hepatocytes is likely to contribute to lowering blood glucose levels in PDX1-VP16-mice.

To confirm that the hepatocytes were secreting insulin, serum levels of immunoreactive insulin in these mice on day 40 after adenoviral administration were measured. In LacZ-mice, STZ treatment induced severe insulinopenia: fasting serum insulin levels were less than 40 pg/ml (Fig. 1D), resulting in severe hyperglycemia. Adenoviral administration of the wt-PDX1 gene slightly increased serum insulin levels. In contrast, PDX1-VP16 adenoviral administration resulted in a substantial increase in serum insulin levels, i.e., more than 6-fold (Fig. 1D). On the other hand, fasting serum insulin levels in the control C57Bl/6N mice of the same age, without STZ treatment, were 340.7 ± 29.9 pg/ml ($n = 6$). Thus, hepatic PDX1-VP16 expression improved fasting serum insulin levels to approximately two-thirds those in normal mice. These data suggest that transient PDX1-VP16 expression in the liver exerted sustained and stronger effects in terms of production and secretion of insulin as compared with wt-PDX1 expression, resulting in the reversal of STZ-induced hyperglycemia.

Oral glucose tolerance tests were performed using LacZ-mice, wt-PDX1-mice, and PDX1-VP16-mice on day 40 (Fig. 2A). STZ-treated LacZ-mice exhibited hyperglycemia: more than 450 mg/dl throughout the

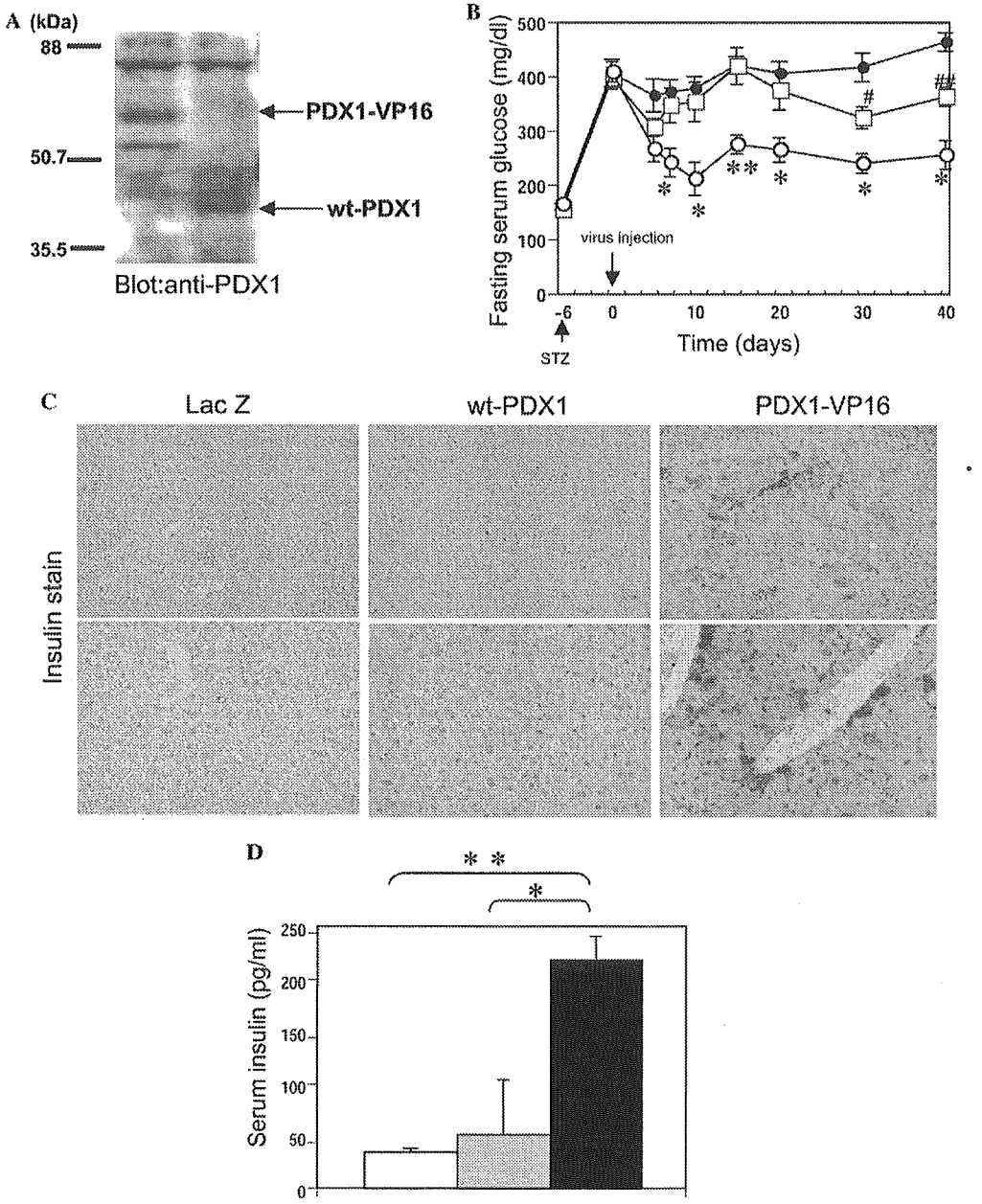

Fig. 1. Effects of wt-PDX1 and PDX1-VP16 adenoviral gene therapy on STZ-induced diabetic mice. (A) Liver lysates from STZ-mice infused with 2×10^8 pfu/body of adenovirus containing wt-PDX1 (left lane) or PDX1-VP16 (right lane) were immunoblotted with anti-PDX1 antibody. (B) Fasting blood glucose levels of STZ-mice treated with LacZ adenovirus (closed circle; $n = 13$), wt-PDX1 adenovirus (open square; $n = 8$) or PDX1-VP16 adenovirus (open circle; $n = 15$). Amount of injected adenoviruses was 2×10^8pfu/body in all experiments. (C) Liver sections from LacZ-mice (left panels), wt-PDX1-mice (middle panels), and PDX1-VP16-mice (right panels) on day 40 after adenoviral treatment were immunostained with anti-insulin antibody. Original magnification 100× (upper panels) and 200× (lower panels). (D) Fasting serum insulin levels 40 days after adenoviral treatment with LacZ (open bar; $n = 7$), wt-PDX1 (gray bar; $n = 8$), or PDX1-VP16 (black bar; $n = 7$) adenovirus. Data are presented as means ± SEM. $^*P < 0.05$, $^{**}P < 0.01$ versus wt-PDX1, $^{\#}p < 0.05$, and $^{\#\#}p < 0.01$ versus LacZ, assessed by unpaired t test.

tests. In PDX1-VP16-mice, glucose levels throughout the tests were significantly lower than those in wt-PDX1-mice. The blood glucose levels peaked at 30 min after glucose load and thereafter tended to fall, although the reversal was incomplete at 120 min. These findings suggest that, in PDX1-VP16-mice, glucose-responsive insulin secretion from the liver is involved in lowering post-prandial blood glucose levels but is not enough to rapidly reverse a rise in blood glucose levels after a glucose load, in contrast to that from the pancreas by β cells.

Using HDAD, PDX1 expression in the liver reportedly induces expression of exocrine enzymes in insulin-producing cells in the liver and causes severe hepatitis. It has also been reported that, in transgenic mice expressing PDX1 ectopically in the liver, not only insulin but

Table 1
Distribution of blood glucose levels in each treatment group

Blood glucose (mg/dl)	100–200	200–300	300–400	400–500	500–600
LacZ (%)	0	0	8	69	23
wt-PDX1 (%)	0	12	50	38	0
PDX1-VP16 (%)	27	47	13	13	0

Blood glucose levels were determined 40 days after each adenoviral treatment. Blood glucose levels of mice before the adenoviral treatment (6 days after STZ injection) were all above 300 mg/dl. (Lac Z; $n = 13$, wt-PDX1; $n = 8$, and PDX1-VP16; $n = 15$.)

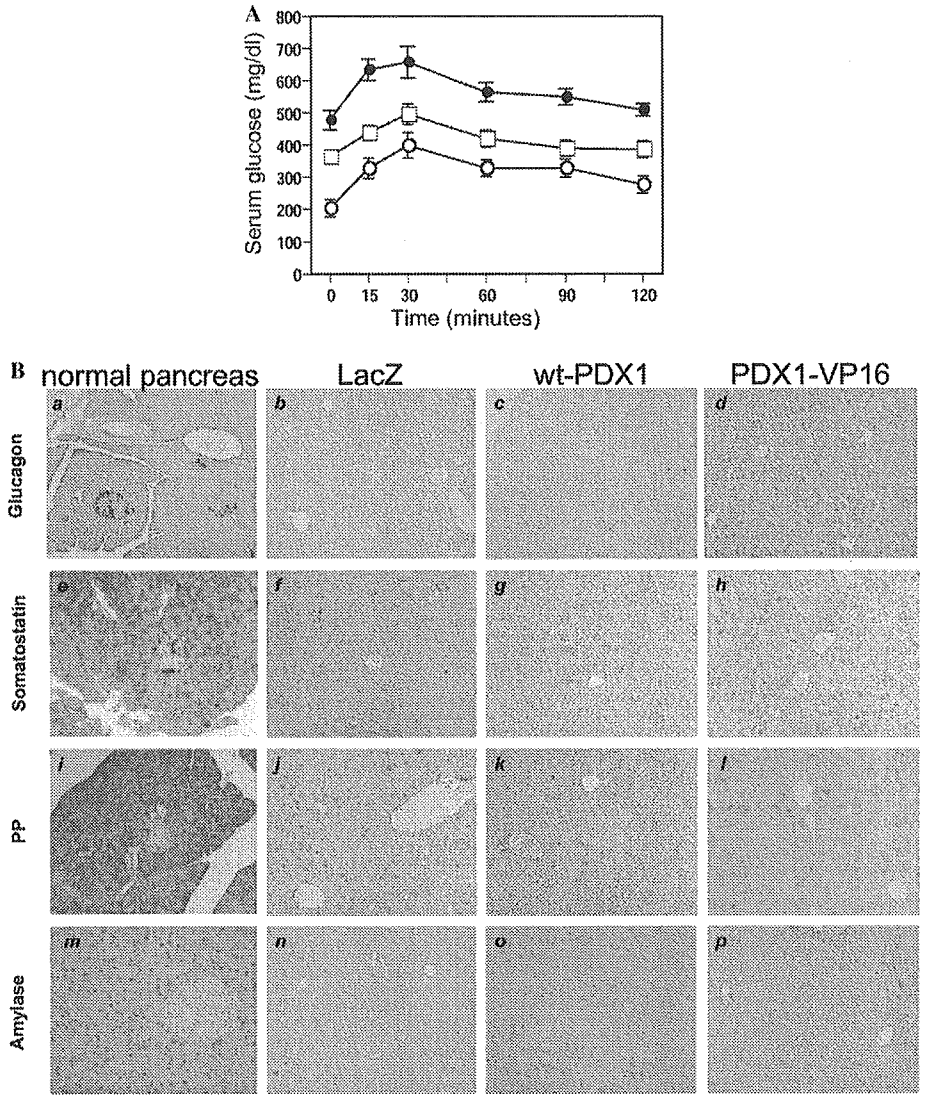

Fig. 2. Effects of wt-PDX1 and PDX1-VP16 adenoviral gene therapy on blood glucose levels after a glucose load, and glucagon, somatostatin, pancreatic polypeptide, and amylase expressions. (A) Blood glucose levels during oral glucose tolerance testing (1 g/kg body weight) in LacZ-mice (closed circle; $n = 7$), wt-PDX1-mice (open square; $n = 8$), and PDX1-VP16-mice (open circle; $n = 7$) on day 40 after adenovirus administration. Data are presented as means ± SEM. (B) immunohistochemical staining of livers from LacZ-mice (b,f,j,n), wt-PDX1-mice (c,g,k,o), and PDX1-VP16-mice (d,h,l,p) with glucagon (b–d), somatostatin (f–h), pancreatic polypeptide (j–l) or amylase (n–p) antibody. Sections of normal pancreas were used as positive controls for each staining procedure (a,e,i,m). Original magnification 100×.

also other endocrine hormones as well as pancreatic exocrine genes are expressed, resulting in dysmorphogenesis and hepatic failure [10]. In contrast, in the present study, adenovirus-mediated transduction of the wt-PDX1 or the PDX1-VP16 gene into the liver did not induce lobe structural abnormalities or substantial infiltration of inflammatory cells (Fig. 2B). Furthermore, using immunohistochemistry, no immunoreactivity against glucagon

or somatostatin was detected in livers from wt-PDX1-mice and PDX1-VP16-mice. In addition, in these livers there was no detectable production of amylase, a pancreatic exocrine enzyme (Fig. 2B), which may explain the normal morphogenesis in our experimental animals. On the other hand, pancreatic polypeptide was expressed in livers from PDX1-VP16-mice, and in those from wt-PDX1-mice though to a lesser extent. These results demonstrate that transient expression of PDX1-VP16 alters the character of hepatocytes to preferentially produce insulin and pancreatic polypeptide, but not other endocrine hormones or exocrine enzymes.

Adenoviral gene transfer induced gene expression for 1 week but, after 2 weeks, this expression reportedly disappeared [22]. However, in the present study, the blood glucose lowering effects and hepatic insulin expression persisted for at least 40 days. Therefore, the time course of PDX1 protein expression levels was examined. As shown in Fig. 3A, immunoblotting using anti-VP16 activation domain antibody revealed PDX1-VP16 protein to be expressed on day 3 but expression was markedly decreased on day 7, and undetectable on day 21. Thus, even after disappearance of VP16-PDX1 expression, hepatocytes expressed insulin, resulting in lowering of blood glucose levels. Interestingly, immunoblotting using anti-PDX1 antibody showed that endogenous PDX1 protein, which had the same molecular weight as wt-PDX1, came to be expressed on day 21. Thus, transient expression of PDX1-VP16 endowed hepatocytes with certain pancreatic β cell features and endogenous PDX1 expression is likely to maintain the insulin-producing function of these cells.

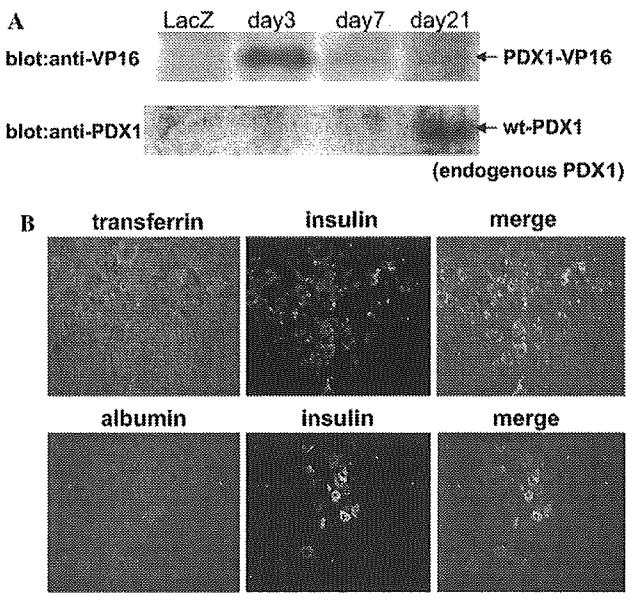

Fig. 3. Treatment with PDX1-VP16 adenovirus induced persistent expression of endogenous PDX1 but albumin and transferrin were co-expressed in insulin-expressing cells. (A) Liver lysates from PDX1-VP16 mice at different time points after adenoviral treatment were immunoblotted with anti-VP16 (upper panel) or anti-PDX1 (lower panel) antibody. (B) Liver sections from PDX1-VP16 mice on day 40 were double-immunostained with insulin (middle panels) and transferrin (upper-left panels) or albumin (lower-left panels) antibodies. Right panels represent the merged images.

To determine whether the insulin-producing cells in the liver had completely transdifferentiated and lost their hepatocytic character, liver sections from PDX1-VP16 mice on day 40 were immunostained with insulin and transferrin (upper panels in Fig. 3B) or albumin (lower panels in Fig. 3B). Fluorescence immunohistochemistry revealed that insulin-producing cells in the liver also expressed transferrin and albumin. Expression levels of these liver-specific proteins were not substantially decreased as compared with non-insulin-producing cells around the insulin-producing cells. These findings suggest functional hepatocyte-specific characteristics are maintained in insulin-producing cells in the liver. Thus, these hepatocytes were not completely converted to pancreatic cells.

Discussion

In the present study, administration of recombinant adenovirus containing an activated form of PDX1 efficiently induced insulin production in hepatocytes, resulting in reversal of STZ-induced hyperglycemia. The effects were sustained even when exogenous protein expression was no longer detectable. In turn, endogenous PDX1 protein came to be expressed in hepatocytes, which is likely to be the mechanism underlying the sustained effects. On the other hand, albumin and transferrin expressions were observed in insulin-producing cells, suggesting the maintenance of hepatocyte-specific characteristics.

Ferber et al. [7] reported that administration of wt-PDX1 adenovirus at 2×10^9 pfu/mouse ameliorates STZ-induced hyperglycemia but the observed period was very short (no more than 10 days). The same research group also reported the long-term effects of PDX1 gene transfer but the titer of recombinant adenovirus used was relatively high ($1–5 \times 10^{10}$ pfu/mouse) [12]. Such high titers may result in liver damage due to adenoviral toxicity. In the present study, to avoid adenoviral toxicity, recombinant adenoviruses were injected at a titer as low as 2×10^8 pfu. With such a small adenoviral delivery, the wt-PDX1 adenovirus exerted very small effects on insulin and glucose levels, whereas PDX1-VP16 adenovirus substantially increased insulin levels and reversed STZ-induced hyperglycemia. These findings suggest that constitutive activation of PDX1 overcomes the inefficiency associated with low expression levels of PDX1 proteins. Thus, adenoviral transfer of the PDX1-VP16 gene into the liver would presumably be safer than wt-PDX1 gene therapy.

HDAD-mediated PDX1 expression in the liver reportedly causes severe hepatitis including marked inflammatory cell infiltration with focal necrosis associated with expression of pancreatic exocrine genes [10]. In addition, conditional transgenic mice generated by crossing CAG-CAT-PDX1 mice with alb-Cre recombinase-mice also displayed functional liver failure with hepatic expression of exocrine enzymes [11]. In these two models, exogenous PDX1 expression is persistent. Transgenes delivered by HDADs are expressed for long periods exceeding several months. In conditional transgenic mice [11], cells, in which the albumin promoter had once been activated, permanently expressed PDX1 driven by the CAG promoter. These findings suggest that high and persistent expression of PDX1 induces exocrine enzyme expression and thereby liver failure. In the present study, exogenous gene expressions of wt-PDX1 and PDX1-VP16 were transient and expression levels were relatively low on day 7 (Fig. 3A). Thus, transient expression appears to be important for endowing hepatocytes with certain features of pancreatic β cells, but not of exocrine cells.

It is noteworthy that exogenous, transient expression of PDX1-VP16 induced prolonged expression of endogenous PDX1 which apparently contributed to persistent insulin production with hepatocytic features. Ber et al. also reported that rat PDX1 gene transduction using first-generation adenovirus induced persistent endogenous (murine) PDX1 expression. Thus, transient expression of wt-PDX1, and more efficiently PDX1-VP16, may induce persistent and low-level expression of endogenous PDX1. In the adult pancreas, persistent but low-level expression of PDX1 is detected only in β cells [3] and PDX1 expression is required for maintaining normal pancreatic β cell function [6]. These observations suggest that persistent, low-level expression of PDX1 is involved in preferential production of insulin and pancreatic popypeptide in hepatocytes.

In transgenic *Xenopus* tadpoles expressing Xlhbox8 (*Xenopus* homolog of PDX1) carrying the VP16 activation domain under a transthyretin promoter, part or all of the liver is reportedly converted to pancreatic tissue without expression of liver-specific gene products, suggesting complete conversion of hepatocytes to pancreatic cells [14]. In contrast, in the present study, insulin-producing cells in the liver in PDX1-VP16 mice also expressed albumin and transferrin, which suggests preservation of hepatocytic functions. This discrepancy may be explained by the differences between amphibian and mammalian cells. Alternatively, the conversion may occur during embryonic differentiation, while, in adult and differentiated hepatocytes, complete transdifferentiation into pancreatic endocrine or exocrine cells would be difficult to achieve even with PDX1-VP16 expression. Although intensive research is necessary to unravel the precise mechanisms underlying transdifferentiation, the partial conversion induced by PDX1-VP16 expression in adult hepatocytes has practical applications, since loss of hepatocytic functions may result in liver failure. Furthermore, incomplete transdifferentiation could prevent the generated insulin-producing cells from being attacked by a destructive autoimmune response in type 1 diabetics.

Acknowledgments

We thank Dr. H. Kanamori (University of Tokyo) for the generous gift of the VP16 gene. We also thank Ms. I. Sato, K. Kawamura, and M. Hoshi for technical support. This work was supported by a Grant-in-Aid for Scientific Research (B2, 15390282), a Grant-in-Aid for Exploratory Research (15659214) to H. Katagiri, and a Grant-in-Aid for Scientific Research (13204062) to Y. Oka from the Ministry of Education, Science, Sports and Culture of Japan. This work was also supported by Tohoku University 21st Century COE Program "CRESCENDO" to J. Imai, J. Gao, and H. Katagiri.

References

[1] A.M. Shapiro, J.R. Lakey, E.A. Ryan, G.S. Korbutt, E. Toth, G.L. Warnock, N.M. Kneteman, R.V. Rajotte, Islet transplantation in seven patients with type 1 diabetes mellitus using a glucocorticoid-free immunosuppressive regimen, N. Engl. J. Med. 343 (2000) 230–238.

[2] G. Deutsch, J. Jung, M. Zheng, J. Lora, K.S. Zaret, A bipotential precursor population for pancreas and liver within the embryonic endoderm, Development 128 (2001) 871–881.

[3] H. Ohlsson, K. Karlsson, T. Edlund, Ipf1, a homeodomain-containing transactivator of the insulin gene, EMBO J. 12 (1993) 4251–4259.

[4] M.F. Offield, T.L. Jetton, P.A. Labosky, M. Ray, R.W. Stein, M.A. Magnuson, B.L. Hogan, C.V. Wright, Pdx-1 is required for pancreatic outgrowth and differentiation of the rostral duodenum, Development 122 (1996) 983–995.

[5] J. Jonsson, L. Carlsson, T. Edlund, H. Edlund, Insulin-promoter-factor 1 is required for pancreas development in mice, Nature 371 (1994) 606–609.

[6] U. Ahlgren, J. Jonsson, L. Jonsson, K. Simu, H. Edlund, Beta-cell-specific inactivation of the mouse ipf1/pdx1 gene results in loss of the beta-cell phenotype and maturity onset diabetes, Genes Dev. 12 (1998) 1763–1768.

[7] S. Ferber, A. Halkin, H. Cohen, I. Ber, Y. Einav, I. Goldberg, I. Barshack, R. Seijffers, J. Kopolovic, N. Kaiser, A. Karasik, Pancreatic and duodenal homeobox gene 1 induces expression of insulin genes in liver and ameliorates streptozotocin-induced hyperglycemia, Nat. Med. 6 (2000) 568–572.

[8] A. Grapin-Botton, A.R. Majithia, D.A. Melton, Key events of pancreas formation are triggered in gut endoderm by ectopic expression of pancreatic regulatory genes, Genes Dev. 15 (2001) 444–454.

[9] R.S. Heller, D.A. Stoffers, M.A. Hussain, C.P. Miller, J.F. Habener, Misexpression of the pancreatic homeodomain protein idx-1 by the hoxa-4 promoter associated with agenesis of the cecum, Gastroenterology 115 (1998) 381–387.

[10] H. Kojima, M. Fujimiya, K. Matsumura, P. Younan, H. Imaeda, M. Maeda, L. Chan, Neurod-betacellulin gene therapy induces islet neogenesis in the liver and reverses diabetes in mice, Nat. Med. 9 (2003) 596–603.
[11] T. Miyatsuka, H. Kaneto, Y. Kajimoto, S. Hirota, Y. Arakawa, Y. Fujitani, Y. Umayahara, H. Watada, Y. Yamasaki, M.A. Magnuson, J. Miyazaki, M. Hori, Ectopically expressed pdx-1 in liver initiates endocrine and exocrine pancreas differentiation but causes dysmorphogenesis, Biochem. Biophys. Res. Commun. 310 (2003) 1017–1025.
[12] I. Ber, K. Shternhall, S. Perl, Z. Ohanuna, I. Goldberg, I. Barshack, L. Benvenisti-Zarum, I. Meivar-Levy, S. Ferber, Functional, persistent, and extended liver to pancreas transdifferentiation, J. Biol. Chem. 278 (2003) 31950–31957.
[13] S. Dutta, M. Gannon, B. Peers, C. Wright, S. Bonner-Weir, M. Montminy, Pdx:Pbx complexes are required for normal proliferation of pancreatic cells during development, Proc. Natl. Acad. Sci. USA 98 (2001) 1065–1070.
[14] M.E. Horb, C.N. Shen, D. Tosh, J.M. Slack, Experimental conversion of liver to pancreas, Curr. Biol. 13 (2003) 105–115.
[15] H. Mizuguchi, M.A. Kay, Efficient construction of a recombinant adenovirus vector by an improved in vitro ligation method, Hum. Gene Ther. 9 (1998) 2577–2583.
[16] H. Mizuguchi, M.A. Kay, A simple method for constructing e1- and e1/e4-deleted recombinant adenoviral vectors, Hum. Gene Ther. 10 (1999) 2013–2017.
[17] T. Anno, S. Uehara, H. Katagiri, Y. Ohta, K. Ueda, H. Mizuguchi, Y. Moriyama, Y. Oka, Y. Tanizawa, Overexpression of constitutively activated glutamate dehydrogenase induces insulin secretion through enhanced glutamate oxidation, Am. J. Physiol. Endocrinol. Metab. 286 (2004) E280–E285.
[18] H. Katagiri, T. Asano, H. Ishihara, K. Inukai, Y. Shibasaki, M. Kikuchi, Y. Yazaki, Y. Oka, Overexpression of catalytic subunit p110alpha of phosphatidylinositol 3-kinase increases glucose transport activity with translocation of glucose transporters in 3t3-l1 adipocytes, J. Biol. Chem. 271 (1996) 16987–16990.
[19] I. Sadowski, J. Ma, S. Triezenberg, M. Ptashne, Gal4-vp16 is an unusually potent transcriptional activator, Nature 335 (1988) 563–564.
[20] S.J. Triezenberg, R.C. Kingsbury, S.L. McKnight, Functional dissection of vp16, the trans-activator of herpes simplex virus immediate early gene expression, Genes Dev. 2 (1988) 718–729.
[21] Y. Ishigaki, S. Oikawa, T. Suzuki, S. Usui, K. Magoori, D.H. Kim, H. Suzuki, J. Sasaki, H. Sasano, M. Okazaki, T. Toyota, T. Saito, T.T. Yamamoto, Virus-mediated transduction of apolipoprotein e (apoe)-sendai develops lipoprotein glomerulopathy in apoe-deficient mice, J. Biol. Chem. 275 (2000) 31269–31273.
[22] M.J. Peeters, G.A. Patijn, A. Lieber, L. Meuse, M.A. Kay, Adenovirus-mediated hepatic gene transfer in mice: comparison of intravascular and biliary administration, Hum. Gene Ther. 7 (1996) 1693–1699.

Available online at www.sciencedirect.com

SCIENCE DIRECT®

Advanced Drug Delivery Reviews 57 (2005) 781–802

Advanced DRUG DELIVERY Reviews

www.elsevier.com/locate/addr

Approaches to improving the kinetics of adenovirus-delivered genes and gene products

Zhi-Li Xu[a], Hiroyuki Mizuguchi[b,*], Fuminori Sakurai[b], Naoya Koizumi[b,c], Tetsuji Hosono[a], Kenji Kawabata[b], Yoshiteru Watanabe[d], Teruhide Yamaguchi[a], Takao Hayakawa[c]

[a]*Division of Cellular and Gene Therapy Products, National Institute of Health Sciences, Tokyo 158-8501, Japan*
[b]*Project III, National Institute of Health Sciences, Osaka Branch, 7-6-8 Asagi, Saito, Ibaraki, Osaka 567-0085, Japan*
[c]*National Institute of Health Sciences, Tokyo 158-8501, Japan*
[d]*Department of Pharmaceutics and Biopharmaceutics, Showa Pharmaceutical University, Tokyo 194-8543, Japan*

Received 25 December 2003; accepted 18 December 2004

Abstract

Adenovirus (Ad) vectors have been expected to play a great role in gene therapy because of their extremely high transduction efficiency and wide tropism. However, due to the intrinsic deficiency of their immunogenic toxicities, Ad vectors are rapidly cleared from the host, transgene expression is transient, and readministration of the same serotype Ad vectors is problematic. As a result, Ad vectors are continually undergoing refinement to realize their potential for gene therapy application. Even after 1999, when a patient fatally succumbed to the toxicity associated with Ad vector administration at a University of Pennsylvania (U.S.) experimental clinic, enthusiasm of gene therapists for Ad vectors has not waned. With great efforts from various research groups, significant advances have been achieved through comprehensive approaches to improving the kinetics of Ad vector-delivered genes and gene products.

Keywords: Immunogenic toxicities; Biodistribution; Cationic liposome; PEGylation; Helper-dependent; Targeting; In-cis acting element; Integration; Regulatable expression

Contents

* Corresponding author. Tel.: +81 72 641 9815; fax: +81 72 641 9816.
E-mail address: mizuguch@nihs.go.jp (H. Mizuguchi).

0169-409X/$ - see front matter © 2005 Elsevier B.V. All rights reserved.
doi:10.1016/j.addr.2004.12.010